


## RESEARCH ARTICLE

# Telomere elongation through hTERT immortalization leads to chromosome repositioning in control cells and genomic instability in Hutchinson-Gilford progeria syndrome fibroblasts, expressing a novel SUN1 isoform

Mehmet U. Bikkul<sup>1</sup> | Richard G. A. Faragher<sup>2</sup> | Gemma Worthington<sup>1</sup> | Peter Meinke<sup>3,4</sup> | Alastair R. W. Kerr<sup>4</sup> | Aakila Sammy<sup>1</sup> | Kumars Riyahi<sup>1</sup> | Daniel Horton<sup>1</sup> | Eric C. Schirmer<sup>4</sup> | Michael Hubank<sup>5</sup> | Ian R. Kill<sup>1</sup> | Rhona M. Anderson<sup>1</sup> | Predrag Slijepcevic<sup>1</sup> | Evgeny Makarov<sup>1</sup> | Joanna M. Bridger<sup>1</sup> 

<sup>1</sup>Genome Engineering and Maintenance Network, Institute for Environment, Health and Societies, Brunel University London, Uxbridge, England

<sup>2</sup>Pharmacy and Biomolecular Sciences, University of Brighton, Brighton, England

<sup>3</sup>Friedrich-Baur-Institut, Klinikum der Universität München, München, Germany

<sup>4</sup>The Wellcome Trust Centre for Cell Biology, Institute of Cell Biology, and Centre for Translational and Chemical Biology, University of Edinburgh, Edinburgh, England

<sup>5</sup>Centre for Molecular Pathology, The Royal Marsden Hospital, London, England

## Correspondence

Joanna M. Bridger, Genome Engineering and Maintenance Network, Institute for Environment, Health and Societies, Brunel University London, Uxbridge, UB8 3PH, England.

Email: joanna.bridger@brunel.ac.uk

## Funding information

Brunel Progeria Research Fund (MEB and GW)

## Abstract

Immortalizing primary cells with human telomerase reverse transcriptase (hTERT) has been common practice to enable primary cells to be of extended use in the laboratory because they avoid replicative senescence. Studying exogenously expressed hTERT in cells also affords scientists models of early carcinogenesis and telomere behavior. Control and the premature ageing disease—Hutchinson-Gilford progeria syndrome (HGPS) primary dermal fibroblasts, with and without the classical G608G mutation have been immortalized with exogenous hTERT. However, hTERT immortalization surprisingly elicits genome reorganization not only in disease cells but also in the normal control cells, such that whole chromosome territories normally located at the nuclear periphery in proliferating fibroblasts become mislocalized in the nuclear interior. This includes chromosome 18 in the control fibroblasts and both chromosomes 18 and X in HGPS cells, which physically express an isoform of the LINC complex protein SUN1 that has previously only been theoretical. Additionally, this HGPS cell line has also become genomically unstable and has a tetraploid karyotype, which could be due to the novel SUN1 isoform. Long-term treatment with the hTERT inhibitor BIBR1532 enabled the reduction of telomere length in the immortalized cells and resulted that these mislocalized internal chromosomes to be located at the nuclear periphery, as assessed in actively proliferating cells.

Taken together, these findings reveal that elongated telomeres lead to dramatic chromosome mislocalization, which can be restored with a drug treatment that results in telomere reshortening and that a novel SUN1 isoform combined with elongated telomeres leads to genomic instability. Thus, care should be taken when interpreting data from genomic studies in hTERT-immortalized cell lines.

## KEYWORDS

BIBR1532, chromosome territories, genomic instability, hTERT, Hutchinson-Gilford progeria syndrome, M-FISH, Q-FISH, SUN1, SUN1 isoform 9, telomeres

**Abbreviations:** CCD, charged couple device; CcFI, corrected calibrated fluorescence; Cy3, Cyanine 3; DAPI, 4', 6-diamidino-2-phenylindole; DMEM, Dulbecco's Modified Eagle's Medium; DMSO, dimethyl sulfoxide; DOP-PCR, degenerate oligonucleotide primed-polymerase chain reaction; FBS, fetal bovine serum; FISH, fluorescence in situ hybridization; FITC, fluorescein isothiocyanate; FTIs, farnesyl transferase inhibitors; HCl, hydrochloric acid; HGPS, Hutchinson-Gilford progeria syndrome; hTERT, human telomerase reverse transcriptase; IQ-FISH, interphase quantitative FISH; KCl, potassium chloride; LAP, lamina-associated polypeptide; LBR, lamin B receptor; LINC, links the nucleoskeleton and cytoskeleton; LY-R, lymphoma radiation-resistant; LY-S, lymphoma radiation-sensitive; M-FISH, multiplex FISH; PNA-FISH, peptide nucleic acid FISH; Rb, retinoblastoma; SDS-PAGE, sodium dodecyl sulfate-PAGE; SSC, saline sodium citrate; TIF, telomere dysfunction-induced foci; TRITC, tetramethylrhodamine.

This is an open access article under the terms of the Creative Commons Attribution-NonCommercial License, which permits use, distribution and reproduction in any medium, provided the original work is properly cited and is not used for commercial purposes.

© 2018 The Authors. *Genes, Chromosomes & Cancer* published by Wiley Periodicals, Inc.

## 1 | INTRODUCTION

Cellular senescence is a state of irreversible cell cycle arrest commonly reached by replicative or cell stress pathways, which can be preceded by signaling of DNA damage and/or telomere shortening.<sup>1–4</sup> Cellular senescence is purported to be a process that occurs *in vivo* to circumvent initiation and uncontrolled growth of cancers.<sup>5</sup> The process of cellular senescence in culture may proceed without telomere erosion<sup>6,7</sup> and could be induced by epigenomic changes such as methylation and inhibition of chromatin deacetylation.<sup>7,8</sup>

Whatever the cause of senescence, the gradual accumulation of nondividing cells throughout the proliferative life spans of cell cultures<sup>9,10</sup> is seen as a major obstacle to the continuous propagation of cells for experimentation. However, it is possible to force cells to immortalize, thus avoiding replicative senescence by introducing the human catalytic subunit-hTERT to activate telomerase *in vitro*<sup>11–13</sup> leading to an infinite extension of the lifespan of an *in vitro* culture,<sup>14</sup> without causing genomic instability.<sup>15</sup> Indeed, human telomerase is reactivated in cancer indicating that telomerase is required for proliferation of cells toward malignancy.<sup>16,17</sup> Thus, just the addition of the telomerase activity and the consequent elongated telomeres does not lead to genomic instability in normal cells but there may be other aspects of genome behavior that could be affected. It should be noted that exogenous telomerase will target the shorter telomeres in preference.<sup>18,19</sup> Indeed, chromosome and gene positioning in interphase nuclei is often altered in cancer cells<sup>20–24</sup> possibly through changes at the epigenomic level, telomere repositioning and/or anchorage to structures within the nucleoskeleton.<sup>20,25</sup>

Chromosome territories<sup>26–28</sup> are nonrandomly positioned in cells<sup>20,29,30</sup> with distinct differences evident between cells in different proliferative states. For example, in human-proliferating fibroblasts more gene-poor chromosome territories are located at the nuclear periphery and gene-rich chromosomes toward the nuclear interior.<sup>31–33</sup> This organization of chromosomes has been confirmed with global genome analysis experimentation revealing more gene-poor sequences located or bound to the nuclear lamina.<sup>34–37</sup> In nonproliferating primary fibroblasts made quiescent either by serum removal or growth confluence, chromosome territories become reorganized into a size distribution with large chromosomes at the nuclear periphery and smaller chromosomes in the nuclear interior.<sup>38–41</sup> With serum removal this reorganization happens rapidly with some chromosomes moving from the periphery to the nuclear interior within several minutes.<sup>38</sup> In replicative senescent cells, chromosome territories also change location to a size distribution, with some subtle differences between quiescent and senescent cells [Mehta et al<sup>39</sup>]. This spatial positioning of the genome is partially regulated through its interaction with, and anchorage through, nuclear structures of the nucleoskeleton such as the nuclear lamina, the LINC complex and integral membrane proteins found at the nuclear periphery,<sup>42</sup> nuclear motor proteins,<sup>43</sup> and nucleoli.<sup>44,45</sup> In addition, the genome may well be organized by other nuclear structures such as nuclear bodies<sup>46–48</sup> or even a possible transnuclear structure such as the nucleoskeleton.<sup>49–51</sup> Telomeres are important structures involved in anchoring the genome and have been shown to have binding interactions with proteins of the nuclear envelope such as lamin A,<sup>52</sup> SUN2,<sup>53</sup>

AKTIP, a telomere associated protein,<sup>54,55</sup> and SUN1; although in SUN1<sup>-/-</sup> mice telomere attachments to the envelope in meiosis were still apparent.<sup>56,57</sup> Telomeres are also seen to be tethered by the internal nuclear nucleoskeleton,<sup>51,58,59</sup> yet it is unclear what they are binding to. It is possible that they bind to internal lamin complexes in the nuclear interior that contain lamin A and Lap2 $\alpha$ ,<sup>60</sup> affected by epigenetic changes.<sup>61,62</sup>

Given the evidence of telomeric binding to various nuclear structures in cells, especially those containing A-type lamins, it is not surprising that in syndromes where there are mutations in A-type lamins, and their binding partners, genome organization is affected.<sup>40,63–68</sup> We and others have demonstrated previously that chromosomes are mislocalized in primary cells derived from patients with laminopathy and carriers, with mutations in lamin A.<sup>40,69</sup> These studies indicate that lamin A is involved in chromosome positioning within interphase nuclei. Previously, we have demonstrated that chromosomes in proliferating primary HGPS cells are mislocalized and are located in nonrandom positions as if the cells were quiescent.<sup>65</sup> Although, recent studies assessing the specific epigenetic clock DNA methylation markings of HGPS cells indicate that they have a prematurely aged signature.<sup>70</sup> However, following treatment with farnesyl transferase inhibitors (FTIs), that prevent the farnesylation of proteins, leads to the mutant lamin A protein—progerin—to have no farnesylation moieties, and so does not become associated aberrantly with the nuclear envelope during mitosis, which restores chromosome territory to that of control cells.<sup>66,71</sup>

In an effort to make HGPS cells more easily cultured and assayable, we employed cells that had been immortalized by hTERT.<sup>72</sup> A control hTERT normal fibroblast line was also employed.<sup>73</sup> Most interestingly we revealed that the inclusion of hTERT into primary control cells altered the position of the territories of chromosome 18 toward the nuclear interior, away from the nuclear periphery, even though the cells were actively proliferating. Two HGPS cell lines also displayed chromosome 18 territories toward the nuclear interior, however, this is normal for HGPS cells.<sup>40,66</sup> Most surprisingly the atypical HGPS cell line, without the classical G608G mutation in the lamin A gene (*LMNA*) displayed genomic instability, particularly aneuploidy, with, in addition, the chromosome X territories located in the nuclear interior. We normally use chromosome X as a control chromosome very often as both copies are always found at the nuclear periphery in our assays. In conclusion, telomere elongation via hTERT has led to chromosome misplacement.

In the treatment of several cancer lines it was demonstrated that a drug called BIBR1532 can repress telomerase activity and cause tumor cell growth arrest without triggering acute cytotoxicity.<sup>74</sup> We found that over time in culture BIBR1532 also permitted telomeres to return to a normal length, with the culture also beginning to contain nonproliferating Ki67 negative cells. Excitingly, this treatment also restored proper chromosome positioning in the immortalized control cells for chromosome 18 and in the HGPS cell with the unknown mutation for chromosome X. Further analysis of this HGPS cell line with the unknown mutation revealed that there was a lower amount of lamin B receptor and SUN1 present at the nuclear envelope. Exome and RNA sequencing of the T08 cells has revealed that this cell line has normal lamin B receptor (LBR) alleles, as well as normal sequences

for all known nuclear envelope proteins; but had an isoform of SUN1 that has not been seen *in vivo* before and is not recognized by available antibodies. This suggests that SUN1 could be important in anchoring chromosome X territories and the newly observed isoform *in vivo* in combination with immortalization by hTERT leads to genomic instability.

## 2 | MATERIALS AND METHODS

### 2.1 | Cell culture and BIBR1532 drug treatment

The NB1 primary human dermal fibroblast cell line<sup>73</sup> was immortalized with hTERT plasmid (a kind gift from Prof Robert Weinstein) and named NB1T.<sup>75</sup> The Hutchinson-Gilford progeria syndrome human dermal fibroblasts AG06297 and AG08466 were purchased from Coriell USA and also immortalized with hTERT,<sup>72</sup> then named T06 and T08, respectively. All fibroblasts were derived from skin biopsies for HGPS cells and a neonate foreskin for the control NB1. Prior to immortalization both HGPS cell lines displayed diploid chromosome numbers and AG06297 continued to do so after immortalization. Cells were grown in Dulbecco's Modified Eagles Medium (DMEM) (Invitrogen, UK), with 15% fetal bovine serum (FBS) (Invitrogen), 2% [vol/vol] streptomycin and penicillin antibiotics (Invitrogen) and 200 mM L-glutamine (Invitrogen). NB1T and T08 cells were treated with 10  $\mu$ M of BIBR1532 for 8 weeks and 6 weeks, respectively. Control cells were treated with corresponding solvent (DMSO) concentrations.

### 2.2 | Metaphase chromosome preparations

A volume of 1% colcemid solution was added to each dish 1 hour prior to harvest and incubated in 0.075 M KCl at room temperature for 15 minutes prior to fixation in methanol: acetic acid (3:1 vol/vol). Fixed chromosomes were stained with DAPI and "Metafercell Software" was used for the automated detection and imaging of metaphase spreads.

### 2.3 | Multiplex fluorescence in situ hybridization assay

24-colour karyotyping (multiplex fluorescence in situ hybridization [M-FISH]) was used to paint mitotic chromosomes of the T08 cell line using a modified method of the Metasystems protocol as described previously.<sup>76</sup>

For analysis, metaphase cells were visualized using an 8-position Zeiss Axioplan II fluorescence microscope containing individual filter sets for each component fluor of the Metasystems (Cambridge, UK) probe cocktail plus DAPI. Digital images were captured for M-FISH using a cooled charged-coupled device (CCD) camera (Photometrics Sensys CCD, Tuscon, AZ, USA) coupled to and driven by ISIS (Metasystems). In the first instance, cells were karyotyped and analyzed by enhanced DAPI banding. Detailed paint analysis was then performed by assessing paint coverage for each individual fluor down the length of each individual chromosome, using both the raw and processed images for each fluor channel. A metaphase spread was classified as being apparently normal if all 46 chromosomes were

observed by this process, and subsequently confirmed by the Metasystems M-FISH assignment, to have their appropriate combinatorial paint composition down their entire length.

Structural chromosomal abnormalities were identified as color-junctions down the length of individual chromosomes and/or by the presence of chromosome fragments. The M-FISH paint composition was used to identify the chromosomes involved in the abnormality and assignment of a breakpoint to a specific chromosomal region (pter, p, peri-centromere, q or qter) was based on the DAPI-banding pattern at the M-FISH color junction, the location of the centromere and the size of the painted material on each rearranged chromosome. Abnormalities were described according to International System of Cytogenetic Nomenclature (ISCN 2009).

### 2.4 | Chromosome-positioning assay by 2D FISH

Cells were fixed in ice-cold methanol: acetic acid (3:1, vol/vol, respectively) and dropped onto slides. Aged slides were transferred into a denaturing solution (70% (vol/vol) formamide, 2X saline sodium citrate (SSC) at 70°C for 2 minutes. The slides were plunged into ice-cold 70% ethanol and then passed through the ethanol row.<sup>77</sup>

The chromosome templates 18 and X were made in-house by amplifying flow-sorted chromosome arms (a kind gift from Dr Michael Bittner) by degenerate oligonucleotide-primed polymerase chain reaction (DOP-PCR). The chromosome paints were labelled with biotin-16-dUTP (Roche). The probe was precipitated with ethanol with the addition of human Cot 1 DNA (Roche, Basel, Switzerland), herring sperm DNA and 3 M sodium acetate, pH 5 and then dissolved in hybridization mix (50% formamide, 10% dextran sulfate, 10% 20X SSC, 1% Tween 20 overnight at room temperature. The probes were denatured at 75°C for 5 minutes and then allowed to re-anneal at 37°C. The probes were then applied to the slides, and hybridized at 37°C for at least 18 hours. The slides were washed thrice in buffer A (50% vol/vol formamide, 2X SSC, pH 7.0) preheated to 45°C and then thrice in buffer B (0.1X SSC, pH 7.0), preheated to 60°C. Slides were then transferred to 4X SSC at room temperature and incubated with 100- $\mu$ L blocking solution (4% bovine serum albumin [BSA], w/v) for 10 minutes at room temperature. In order to detect the biotin-labelled probes, each slide was incubated in 100  $\mu$ L of 1:200 diluted streptavidin-cyanine (Cy3) (Amersham Life Science, Little Chalfont, UK) at room temperature for 1 hour. Slides were washed in a 4X SSC solution containing 0.05% Tween 20 in the dark at 42°C for 15 minutes. If required the slides were then incubated with anti-pKi67 antibody (DAKO A0047) to identify proliferating cells for 1 hour at room temperature followed by a secondary antibody swine anti-rabbit (TRITC) (Dako R0156) fluorescein isothiocyanate. Afterward, slides were mounted in Vectashield containing DAPI (Vectorlabs, Murarrie, Australia). All slides were examined using 100X Plan Fluorpar oil immersion lens (Leica) on an Olympus BX41 fluorescence microscope. pKi-67 positive nuclei were selected randomly by following a rectangular scan pattern. Imaging was performed using Digital Scientifics software, the Quips Pathvysion. At least 50 images per slide were captured by Smart Capture 3.00 software and signal position analyzed with an erosion analysis script using IPLab Spectrum software. The erosion analysis script (used with kind permission of Prof.

Wendy Bickmore and Dr. Paul Perry, MRC Human Genetics Unit) was devised to divide each captured nucleus into five concentric shells of equal area, the first shell being at the periphery of the nuclei ending in the interior of the nuclei (fifth shell).<sup>33,77</sup> The erosion script measures the pixel signal intensity of DAPI and the chromosome probe. The percentage chromosome signal intensity measurement per shell was divided by the percentage DNA signal intensity measurement of the same shell in order to normalize the data. Bar charts and SE of the mean (SEM) bars were plotted and calculated using these data. Finally, statistical analyses were performed using unpaired two-tailed and Student's *t* tests. To note in young proliferating cultures of HGPS cells, nuclei do not tend to be misshaped and are normally ellipsoid. If the nuclei do display an abnormal shape they are still included in the erosion analysis and given that the script outlines the nuclei absolutely, with invagination and herniations chromosomes are at the nuclear envelope in an invagination will still be recorded at the nuclear periphery.

## 2.5 | Interphase quantitative fluorescence in situ hybridization

Mouse lymphoma LY-R (radio-resistant) and LY-S (radio-sensitive), NB1 and hTERT (Human Telomerase Reverse Transcriptase) fibroblasts were used for interphase quantitative fluorescence in situ hybridization (IQ-FISH). Mouse lymphoma LY-R (radio-resistant) and LY-S (radio-sensitive) cells were used as a reference to measure telomere length using IQ-FISH. Fixed LY-R, LY-S, NB1, NB1T, and T08 cell suspensions were dropped onto glass microscope slides and were immersed in PBS (pH 7.0) for 15 minutes with agitation. After that the samples were treated with 4% formaldehyde for 2 minutes and washed in PBS three times for 5 minutes each. Slides were then immersed preheated (37°C) pretreatment solution for 10 minutes; a total of 500 µL of pepsin (10% pepsin; Sigma) was mixed with 50 mL of acidified dH<sub>2</sub>O of pH 2 and then added to 50 mL-PBS. The slides were fixed again with 4% formaldehyde for 2 minutes. After washing in PBS the slides were dehydrated in an ethanol row consisting of 70%, 85% and 95% (vol/vol). A Cy3-labelled Oligonucleotide PNA (CCCTAA) 3 probe (Dako) complementary to telomeres was used as per manufacturer's instructions. The samples were washed in 70% formamide, followed by PBS and then dehydrated in ethanol (70%, 90%, and 100%). Slides were mounted in Vectashield. At least 30 interphase cells were analyzed for each cell line in triplicate. A 63X objective on an Axioplan 2 Zeiss fluorescence microscope equipped with a CCD camera and the Smart capture 2 image acquisition software (Digital Scientific, Cambridge, UK) was employed to capture images. IP Lab software was used to measure telomere signal intensity which is proportional to telomere length. The two mouse cell lines, LY-R and LY-S, with long and short telomeres, respectively, were used as calibration standards in order to ensure the accuracy of fluorescence intensity measurement.<sup>78,79</sup> As described in Reference 79, in order to obtain arbitrary unit as "CcFL" representing Corrected Calibrated Fluorescence, the values of telomere fluorescence in cells were generated during the five different measurement sessions. It was shown previously by Q-FISH that the parental L5178Y (LY-R) cell line has

telomere length of 49 kb and the LY-S cell line, derived from the LY-R cell line has telomere length of 7 kb.<sup>80</sup>

## 2.6 | Telomere dysfunction-induced foci (TIF) assay

γ-H2AX antibody detection was combined with the IQ-FISH hybridization. γ-H2AX antibody (dilution of 1:500 in 1% PBS/ FCS, Upstate) solution was incubated for 1 hour at room temperature. Goat anti-mouse (FITC) (diluted 1:64 with 1% PBS/FCS, Sigma-F9006) secondary antibody was employed.

## 2.7 | Indirect immunofluorescence

Cell lines were grown on coverslips and fixed with 3.7% paraformaldehyde [wt/vol] for 7 minutes at room temperature. Subsequently, cells were treated with ice-cold methanol: acetone (M:A = 1:1, vol/vol) for 4 minutes at room temperature. The cells were treated with PBS/FBS mixture (1:500 dilution) at room temperature for 10 minutes and then transferred to a humidified chamber and incubated with one of the following primary antibodies CREST human anti-serum (1:1000, Protein Reference Unit, Royal Hallamshire Hospital, Sheffield), mouse anti-HP1α (1:500, Sigma Aldrich-mab3584), mouse anti-H3me3k9 (1:100, Abcam-ab6001), rabbit anti-H3ME3K27 (1:100 Abcam-SAB480001), rabbit anti-H4Me<sup>3</sup>K20 (1:100, Abcam ab9053), mouse anti-lamin A (1:50, Abcam ab8980-1), rabbit anti-lamin B2 (1:250, Abcam-ab151735), mouse anti-emerin (1:30, NCL-emerin), rabbit anti-LBR (1:500, Abcam-ab32535), rabbit anti-SUN1 (1:100, Abcam-ab124770), rabbit anti-SUN2 (1:50, Abcam-ab124916), mouse anti-NUP153 (1:1000, Abcam-ab24700) at RT for 1 hour or overnight at 4°C. Fluorochrome-conjugated secondary antibodies swine anti-rabbit-TRITC (1:25, Dako R0156), goat anti-human-FITC (1:100, Jackson Human Research), goat anti-mouse-FITC (1:64, Sigma-F9006) and goat anti-mouse-TRITC (1:30, Sigma T-5393) were used. Slides were incubated in the dark for either 30 minutes at 37°C or 1 hour at room temperature. The cells were washed and mounted with Vectashield or Mowiol mountant medium containing DAPI counterstain.

## 2.8 | Western blotting

NB1T, TO6, T08 fibroblast cell lines were cultured for 72 hours and samples for western blotting prepared in 3X SDS sample buffer (100 mM Tris-HCl pH 6.8 (wt/vol), 4% SDS (vol/vol), 0.2% Bromophenol blue (vol/vol), 20% glycerol, 0.2% β-mercaptoethanol (vol/vol)). The samples were boiled at 100°C for 3 minutes and stored at -20°C until needed. Cells were loaded onto mini-protean 4%-20% Tris glycine (Bio-Rad) gels at a concentration of  $2 \times 10^5$  cells per well. "Precision Plus Protein™ All Blue Prestained Protein Standards" (Bio-Rad, Watford, UK) were employed as markers. Proteins were then electrophoretically transferred onto nitrocellulose membrane (Amersham Hybond-Cextra, Amersham Biosciences). Membranes were incubated in blocking solution (4%(wt/vol)) dried milk powder (Marvel) in 1X transfer buffer overnight at 4°C, followed by incubation in primary antibodies in 1% FBS/PBS for 1 hour at RT. Following two washes for 5 minutes each in 1X TBS-Tween 20 (50 mM Tris pH 7.4, 150 mM NaCl, 0.1% Tween

20 (vol/vol)). The primary antibodies used were; rabbit anti-LBR (diluted 1:500, Abcam-ab32535), rabbit anti-SUN1 (diluted 1:1000, Abcam-ab124770), rabbit anti-SUN2 (diluted 1:1000, Abcam-ab124916), mouse anti- $\alpha$ -tubulin (diluted 1:4000, Sigma Aldrich-T5168). The diluted infrared secondary antibodies used for western blotting were: Goat (polyclonal) anti-mouse (diluted 1:15 000, LI-COR 926-32 210), Donkey (polyclonal) anti-rabbit (diluted 1:15 000, LI-COR 926-32 213). Fluorescence intensities were determined using a LiCor Odyssey CCD scanner according to manufacturer's instructions (LiCor Biosciences, Cambridge, UK). In order to analyze and quantify the levels of a range of proteins, ImageJ software was employed.

## 2.9 | Cloning and PCRs

### 2.9.1 | Primers

LBR.f1: ATGCCAAGTAGGAAATTTGCCG; LBR.f2: CTGACATCTGCA GTCATCGG; LBR.r1: CCGATGACTGCAGATGTCAGG; LBR.r2: CAAA TGGCAGCTGGAATTGC; SUN1.f1: GGTTTGAAGTGGTGAACATGG; SUN1.f2: GGACAGTGCCACCACCATG; SUN1.r1: CCCAGAATATCTT CCAAGTGTG; SUN1.r2: TCACTTGACAGTTCGCCATG.

Total RNA was isolated from T08 cells using TRIzol reagent and treated with RNase-free DNase according to the protocol of manufacturer (Thermo Fisher Scientific). Total RNA isolated from T08 cells was converted into cDNA using random hexamer primers and the Superscript III reverse transcriptase as suggested by the manufacturer (Invitrogen).

### 2.9.2 | LBR cloning for sequencing

The longest protein-coding transcript from Ensembl database (LBR-001, ENSG00000143815) corresponding to Q14739 protein in UniProt database was used to design the primers. Two parts of the ORF defined by the pairs of primers (LBR.f1 and LBR.r1; LBR.f2 and LBR.r2) as well as the full-length ORF (LBR.f1 and LBR.r2) were amplified from the cDNA using Phusion Hot Start DNA polymerase (Thermo Fisher Scientific). The largest PCR fragment (LBR.f1 and LBR.r2) was cloned into pJET2.1 vector and three clones were sequenced by GENEWIZ UK Ltd.

### 2.9.3 | SUN1 cloning for sequencing

The longest protein-coding transcript from Ensembl database (SUN1-001, ENSG00000164828) was used to design the primers. The N- and C- parts of the ORF defined by the pairs of SUN1.f1 and SUN1.r1, and of SUN1.f2 and SUN1.r2 primers, respectively, as well as the full-length ORF (SUN1.f1 and SUN1.r2) were amplified from the cDNA using Phusion Hot Start DNA polymerase (Thermo Fisher Scientific). The N- and C- parts of the ORF were independently cloned into pJET2.1 vector and three clones from each set were sequenced by GENEWIZ UK.

## 3 | RESULTS

### 3.1 | Chromosome complement of hTERT-immortalized control and HGPS cells

Transfection with hTERT immortalization is a method used to control and extend the life span of important or difficult to grow primary cells

in many laboratories.<sup>81</sup> The karyotype of hTERT immortalized cells remains normal for many passages.<sup>82,83</sup> However, it is still not clear how artificially lengthened telomeres affect chromosome behavior in cells that have been stably transfected with hTERT. Thus, we wished to investigate chromosome positioning in primary fibroblasts immortalized with hTERT. The cell lines we used were a primary male fibroblast cell line created at Brunel University London NB1s, that were immortalized with the hTERT plasmid and named NB1T.<sup>74</sup> We also wished to analyze hTERT-immortalized HGPS primary cells for effects on the genome of immortalization because progerin, the toxic protein formed in HGPS cells, interacts with telomeres.<sup>84</sup> Thus, we employed an HGPS cell line with the classical G608G mutation and another cell line generated from an HGPS patient with an unknown mutation that is not the G608G alteration found in lamin A.<sup>85</sup> These cells were named T06 and T08, respectively.<sup>86</sup>

Initially, we examined whether the hTERT immortalization had created any genomic instability by analyzing the numbers of metaphase chromosomes in 50-130 metaphases for the three immortalized cell lines. Both NB1T and T06 had normal numbers of chromosomes (Figure 1A,B), whereas the immortalized HGPS cell line T08 displayed genomic instability with a median chromosome number of 80 (Figure 1C,D) including both gains and losses and a wide range of abnormalities when analyzed by multiplex-FISH (Figure 1E, Supporting Information Table S1).

It was pertinent to analyze the telomere lengths in all three cell lines compared to a control of the parental NB1 cell line without hTERT immortalization. This was performed using IQ-FISH<sup>87</sup> and fluorescent PNA telomere probes (Figure 2A-D) and it was revealed that NB1 had telomeres that corresponded to 30 corrected calibrated fluorescence lengths (CcFL) (Figure 2E) whereas the immortalized lines had telomere measurements of 120 CcFL for NB1T, T06, and T08 (Figure 2E). Primary HGPS cells have been shown to have shorter telomeres than age matched controls.<sup>88</sup> To determine if the extended telomeres affected their positioning within interphase, nuclei 50 images with delineated telomeres were analyzed using an erosion script, whereby the nucleus is outlined using the DAPI signal to define the edge of the nuclei. The script then erodes inwards creating five shells of equal area in which the intensity of the fluorescence signal from the PNA telomere probe and the DAPI was measured. The percentage intensity signal of the telomeres was normalized by the percentage DAPI signal for each shell.<sup>33</sup> These data were compared between the primary and immortalized cells (Figure 2F). Intranuclear position of telomeres was found not to be dramatically altered but with some subtle and with significant differences within the interior of the cell nuclei in shell 5 between the control cell line and the immortalized cell lines. Overall, using the erosion analysis there were some evident and significant changes in centromere positioning, especially in shell 1 at the edge of nuclei (Supporting Information Figure S1), but again a dramatic difference was not evident. However, when individual territories of chromosomes normally positioned at the nuclear periphery in proliferating human dermal fibroblasts<sup>32,33,38,40</sup> were revealed by FISH dramatically altered nuclear locations became apparent in the hTERT-immortalized cells. In the primary control NB1 cells (Figure 3A,E), positive for the proliferation marker Ki67, the positioning for chromosome 18 was toward the nuclear periphery as has been shown in other

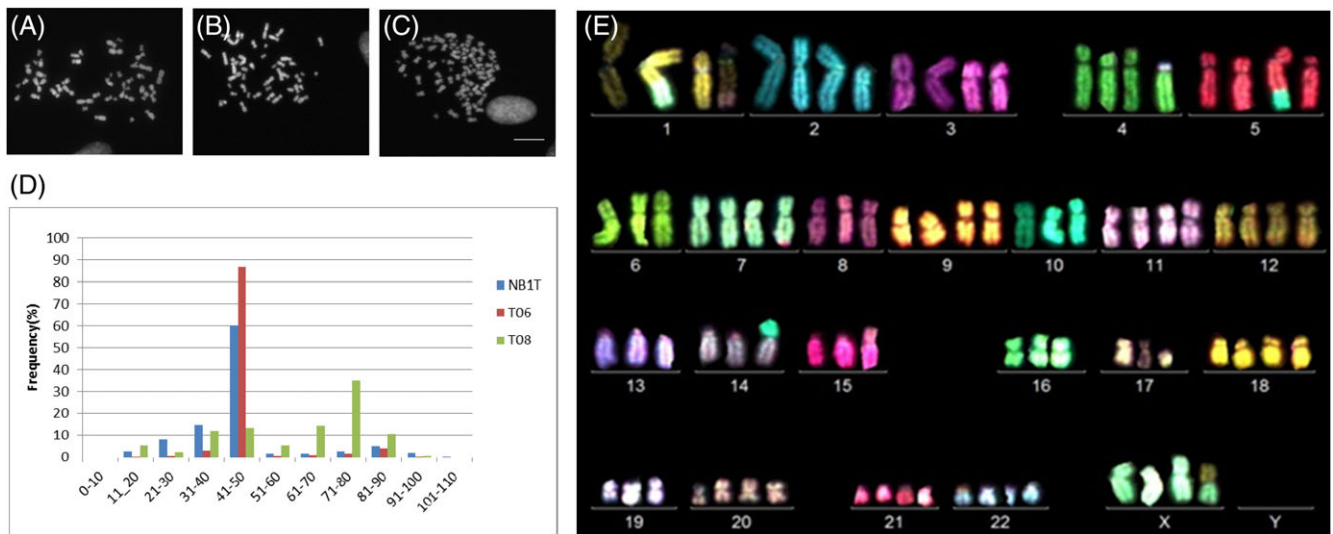


**FIGURE 1** Analysis of chromosomes in the immortalized cell lines. Representative images of metaphase chromosome spreads of NB1T (A), T06 (B) and T08 (C) cells. Scale bar: 5  $\mu$ m. The graph in panel D reveals the number of chromosomes plotted against frequency (%) for each cell line, binned for chromosome number (D). Representative M-FISH karyotype of T08 cell line which is cell 21 displaying genomic instability 83,XXX,t(X;1),ins(1;14),der(1)t(14;1;17),del(2p),del(3p),der(4)t(4;19),der(5)t(5;10), del(5p),-6,der(7)t(7;21),-13,-14,der(14)t(10;14),-15,der(15)t(8;15),-16,del(17q) (E) [Color figure can be viewed at [wileyonlinelibrary.com](http://wileyonlinelibrary.com)]

proliferating human dermal fibroblast studies, with the chromosome signal more evidently distributed in the outer shells 1 and 2, signifying the nuclear periphery. On contrary, chromosome 18 territories, in all hTERT-immortalized cell lines, were located in the nuclear interior (Figure 3B-D, F-H), with signals predominantly in shells 4 and 5. This is normal for primary HGPS-proliferating fibroblasts<sup>40,66</sup> and has been shown for

AG06297 the parental line of T06<sup>40</sup> and is also the case for AG08466 the parental line of T08 (Supporting Information Figure S2) but not proliferating primary control fibroblasts.<sup>33,40,66</sup> Most surprisingly, chromosome X territories, a chromosome we have found only at the nuclear periphery in primary control and HGPS cells including the primary parental line of T08, AG08466 (Supporting Information Figure S2), were also located

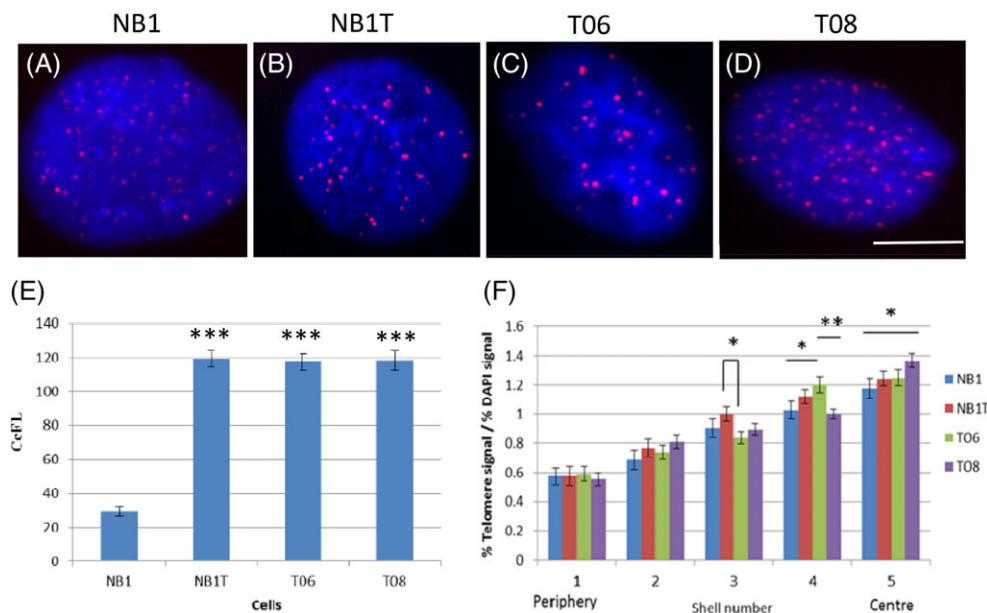


**FIGURE 2** Telomere distribution in the immortalized cell lines. Representative digital images of NB1, NB1T, T06 and T08 cells in interphase after hybridization with cy3-conjugated telomeric peptide nucleic acid (PNA) oligonucleotides (A, B, C, D, respectively) in red and nuclear DNA in blue. Corrected calibrated fluorescence (CcFL) telomere signal intensity for NB1T, T06, and T08 cells relative to the control NB1 cell line (E). \* $P < 0.05$ ; \*\* $P < 0.01$ ; \*\*\* $P < 0.001$ . Error bars represent SE of the mean (SEM). F displays the nuclear position of the telomeres in NB1, NB1, T06, and T08 cells after erosion analysis<sup>33,77</sup> measuring the percentage of the cy3 telomere signal (%), normalized by the percentage of DAPI signal, over five concentric shells of equal area from the nuclear periphery to interior. The x-axis displays the shells from 1 to 5 (left to right), with 1 being the most peripheral shell and 5 being the most internal shell. The y-axis shows the normalized signal (%)/DAPI (%), error bars representing the SE of mean (SEM). Significant differences are denoted by stars (\* $P \leq 0.05$ ; \*\* $P \leq 0.01$ ) (B). Scale bar = 5  $\mu$ m [Color figure can be viewed at [wileyonlinelibrary.com](http://wileyonlinelibrary.com)]

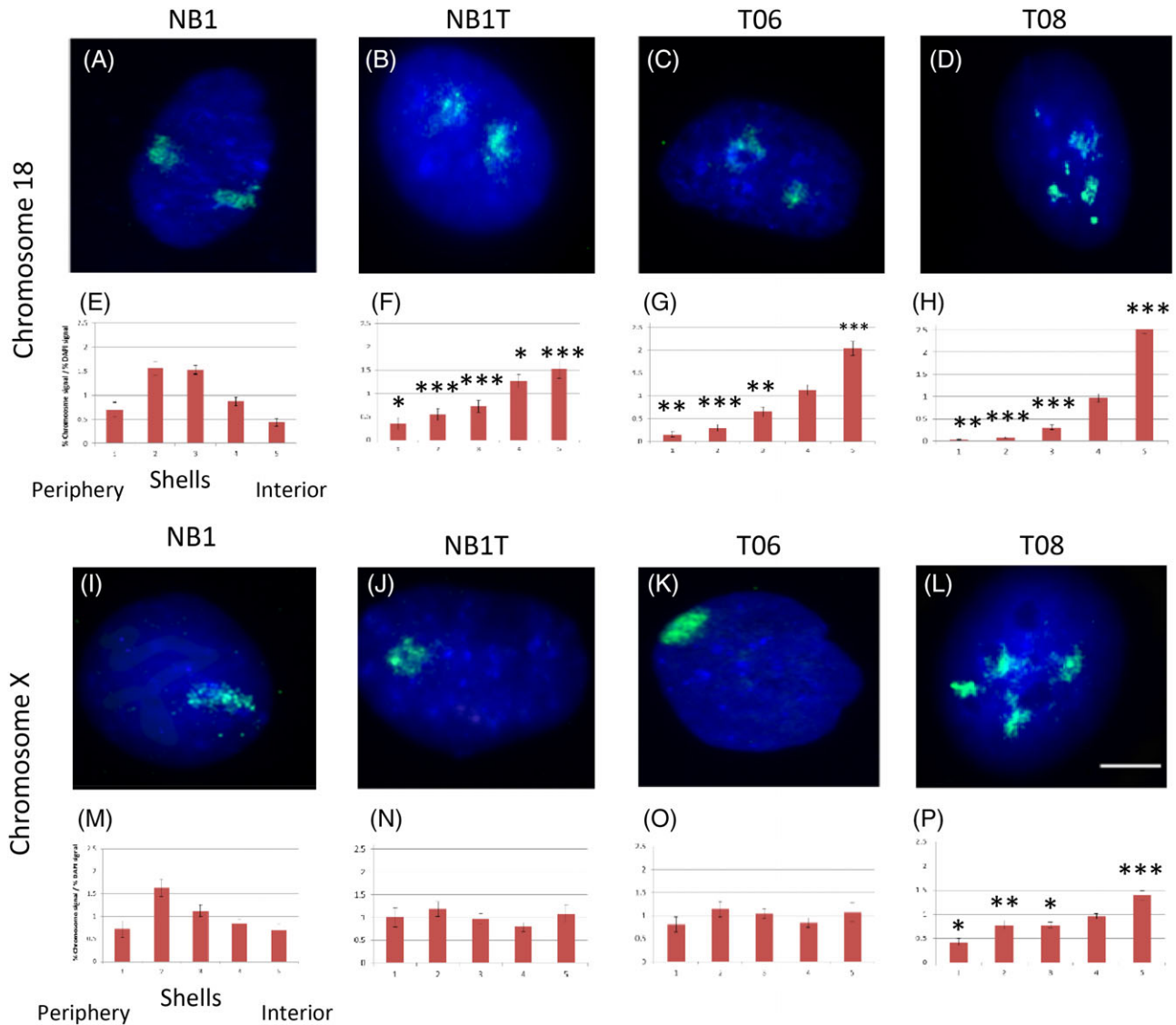


**FIGURE 3** Nuclear locations of chromosome territories. Representative images displaying examples of peripheral, intermediate, and internal positioned chromosome territories in proliferating NB1, NB1T, T06, and T08 cell lines for chromosome 18 (A–D) and chromosome X (I–L). Fibroblasts were subjected to 2D-FISH using whole chromosome painting probes specific to chromosomes 18 and X. The probes were labeled with biotin by degenerate oligonucleotide primed-polymerase chain reaction (DOP-PCR) and detected using streptavidin conjugated to cyanine 3 (colored green) and the nuclei were counterstained with DAPI (blue). Scale bar: 5  $\mu$ m. The bar charts in panels E–H (chromosome 18) and M–P (chromosome X) display the distribution of the chromosome signal in 50–55 nuclei for each chromosome for as analyzed by erosion analysis for NB1, T06, and T08 cells. The x-axis displays the shells from 1 to 5 (left to right) with 1 being the most peripheral shell and 5 being the most internal shell. The y-axis shows chromosome signal (%) / DAPI (%) signal. Bars represent the mean normalized proportion (%) of chromosome signal for each human chromosome. Error bars represent SEM [Color figure can be viewed at [wileyonlinelibrary.com](http://wileyonlinelibrary.com)]

away from the nuclear edge in the HGPS T08 cells but not the other two hTERT-immortalized cell lines, such as NB1T and T06 (Figure 3L,P). Two other chromosomes that were analyzed at the same time (see Supporting Information Figure S3) were chromosomes 10 and 13. In NB1T, T06 and T08 chromosome 10 displays an intermediate location in NB1T where it is normally located in control cells<sup>38</sup> and more internal in T06 cells at odds with what we have found before in nonimmortalized HGPS nuclei.<sup>66</sup> Chromosome 13 territories, which behave similarly to chromosome 18 territories, that is, are located at the nuclear periphery in control fibroblasts,<sup>38,40</sup> display a bimodal distribution in NB1T and are skewed toward the interior in T06 cells. In T08, chromosome 13 is away from the nuclear edge but gives a more random distribution (Supporting Information Figure S3).

Overall, these data reveal that hTERT immortalization has indeed affected positioning of chromosomes in normal control cells and in the HGPS cells T08—the HGPS line with an undiscovered mutation. Most notably these chromosomes are 18 and X and so these are the chromosomes that were used to evaluate whether they can be repositioned following telomere erosion.

### 3.2 | Erosion of telomere length by BIBR1532 leads to restoration of chromosome position

To address the hypothesis that telomere length is responsible for the abnormal chromosome positioning, we employed a drug, BIBR1532, which inhibits telomerase activity.<sup>89</sup> A low dose was employed that

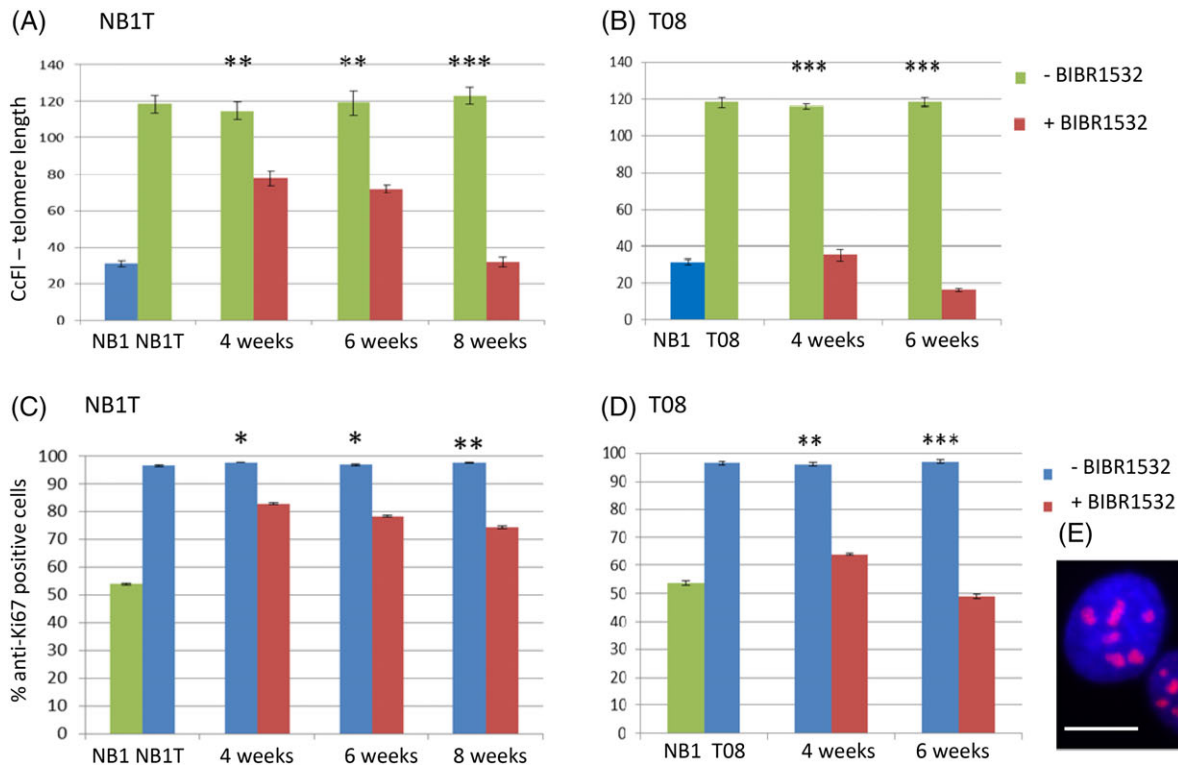


**FIGURE 4** Alterations of telomere length and proliferating cells in hTERT-immortalized cells treated with BIBR1532. Corrected calibrated fluorescence (CcFI) before and after treatment with BIBR1532 NB1T and T08 cell lines relative to the control NB1 cell line. Every 2 weeks from 4 weeks onwards treated and untreated NB1T and T08 cells were measured for telomere fluorescence intensity by performing IQ-FISH (A, B).  $*P \leq 0.05$ ;  $**P < 0.01$ ;  $***P < 0.001$ . Error bars represent SEM. Ki67 in hTERT-immortalized cells treated with BIBR1532. Panel E represents Ki67 nuclei with Ki67 in red and the nuclear DNA stained by DAPI in blue. The fraction of cells displaying positive Ki67 staining was scored with and without the BIBR1532 drug over the culture period of 0–8 weeks and is presented by the graphs (B, D).  $*P \leq 0.05$ ;  $**P < 0.01$ ;  $***P < 0.001$ . Error bars represent SEM [Color figure can be viewed at [wileyonlinelibrary.com](http://wileyonlinelibrary.com)]

was not toxic to cells over a period of 0–8 weeks in culture and did not produce massive amounts of DNA damage, as revealed by  $\gamma$ -H2AX foci and TIFs assay (Supporting Information Figure S4). Telomere lengths were measured every few weeks using IQ-FISH and it was determined that telomere lengths were reduced in NB1T (Figure 4A) and T08 (Figure 4B) cells to similar lengths as found in the NB1 control cells after 8 weeks for NB1T and 6 weeks for T08 cells. These cells were chosen because they both had mislocalized chromosomes. As predicted, the reduction of telomere repeats in the immortalized cells resulted in an increase in senescent cells within the cultures (Figure 4C,D) as demonstrated by the absence of the proliferative marker anti-Ki67 (Figure 4E). The fraction of cells negative for Ki67 increased incrementally over the time span of the experiment, indicating that the immortalization phenotype is satisfactorily reversed by the BIBR1532 drug, creating cells entering senescence.

Samples of cells exposed to BIBR1532 were taken over the long-term culture at 0, 4, 6, and 8 weeks for the NB1Ts and 0, 4, 6 weeks for the T08 cells (Figure 5). For NB1T cells, telomeres reached a similar length to the control NB1 cells after 8 weeks in culture. Chromosome 18 territories were found to be positioned similarly in both cell lines toward the nuclear interior and not at the nuclear periphery (Figure 5B,G). However, over the 8 weeks of BIBR1532 treatment chromosome 18 territories were found to become less internally located in proliferating (Ki67 positive) fibroblasts (Figure 5H,J) and by 8 weeks there was little difference with the NB1 control, with the

chromosomes being in an intermediate position in NB1 and NB1T (+BIBR1532 for 8 weeks), with some statistical differences at the 95% confidence interval in shells 1, 2, 4, and 5. This difference is not comparable to the highly significant differences revealed before the BIBR1532 treatment has reached 8 weeks.

Chromosome X did not change its position significantly in the NB1Ts after the drug treatment (Figure 5K–O and Figure 5P–T), but at 8 weeks of drug treatment the position of X was slightly more peripheral (Figure 5T). Interestingly, no relocation of chromosome 18 territories were observed in the HGPS T08 cells at all after 6 weeks in BIBR1532 (Figure 5U–Z), as was to be expected. However, chromosome X territories were significantly located at the nuclear periphery after the 6 week drug treatment (Figure 5C'F).

### 3.3 | Novel isoform of SUN1 found in T08 cells

Although chromosome 18 is normally positioned in an interior location in HGPS cells,<sup>40,66,71</sup> it is a new finding that the X chromosome territories were also located at the nuclear interior. Thus, we hypothesized that there must be a further factor required to anchor chromosomes at the nuclear periphery in T08s, specifically required by the X chromosomes. This could be an integral membrane/LINC protein, or similar. In order to test this hypothesis, we performed a series of studies with a panel of antibodies recognizing proteins at the nuclear envelope (Figures 6 and S5). Figure 6 displays staining for anti-LBR



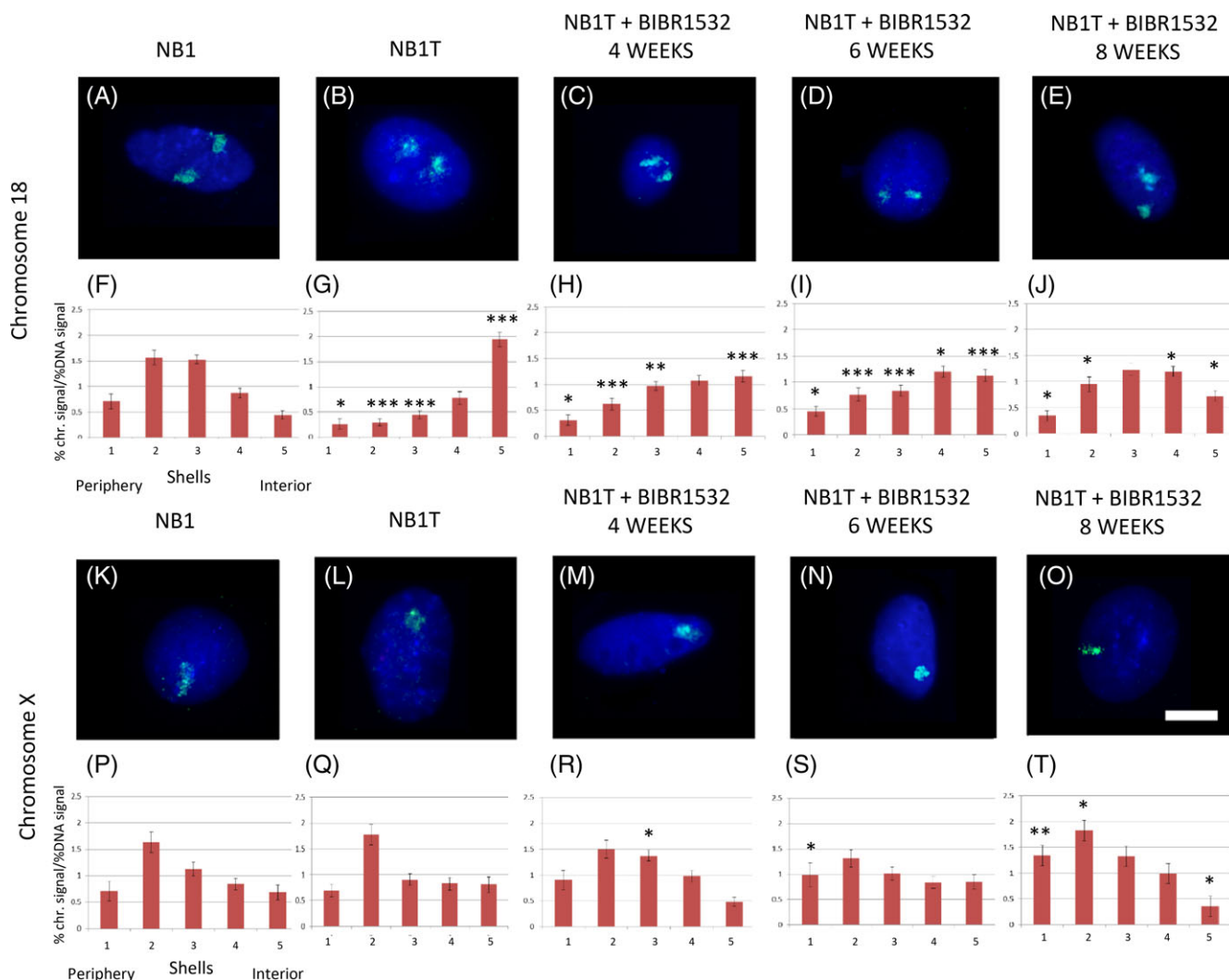


**FIGURE 5** Chromosome repositioning after BIBR1532 treatment. Representative images of the position of chromosome 18 and X within NB1, NB1T, and T08 fibroblasts nuclei before and after drug treatment (A-E, K-O, U-W and A'-C'). Fibroblasts were subjected to 2D-FISH using probes specific to chromosomes 18 and X. Whole chromosome painting probes were labeled with biotin and detected using streptavidin conjugated to cy3 (green) and the nuclei were counterstained with DAPI (blue). Ki-67 staining is not shown in the images. Histograms displaying the nuclear positions of chromosomes 18 and X territories in Ki-67 positive NB1 and NB1T cells before and after drug treatments (F-J) and (P-T). Erosion analyses were performed by ascertaining the distribution of the mean proportion of hybridization signal per chromosome (%), normalized by the percentage of DAPI signal, over five concentric shells of equal area from the nuclear periphery to center. The x-axis displays the shells from 1 to 5 (left to right), with 1 being the most peripheral shell and 5 being the most internal shell. The y-axis shows signal (%)/DAPI (%). Error bars representing SEM were plotted for each shell for each graph (\* $P \leq 0.05$ ; \*\* $P \leq 0.01$ ; \*\*\* $P \leq 0.001$ ; \*\*\*\* $P \leq 0.0001$ ). Scale bar = 5  $\mu\text{m}$ . Bar charts displaying the position of human chromosomes 18 and X territories with Ki-67 positive in T08 cells before and after drug treatments (X-Z and D'-F') [Color figure can be viewed at [wileyonlinelibrary.com](http://wileyonlinelibrary.com)]

(Figure 6A,B) and anti-SUN1 (Figure 6C,D) in which both display a normal distribution at the nuclear rim in NB1T cells, but in T08 cells LBR staining is dull and SUN1 is totally missing from the nuclear rim, localizing to a few small speckles in the nuclear interior (Figure 6D). Assessing LBR and SUN1 levels by western blotting revealed that there are indeed lower levels of LBR in T08 cells by almost one half (Figure 6E) and 12x less SUN1 in T08s when compared to NB1Ts (Figure 6F), normalized by  $\alpha$ -tubulin (Figure 6G). All lamins (A-type and B-type) showed normal levels and distributions in both NB1T and T08 (Supporting Information Figure S5). Others have shown that SUN1 can be involved in HGPS phenotype<sup>90-92</sup> with the lack of SUN1 being beneficial to HGPS cells.<sup>93</sup> On contrary, LBR is overexpressed in skin cells with a classical LMNA G608G mutation.<sup>94,95</sup>

In order to determine if there was a mutation in the T08 cells in either LBR or SUN1, sequencing of open reading frames was performed. All the sequences matched the database entry except two silent substitutions—39V(GTA > GTG) and 87P(CCC > CCT), and one mutation—154S(AAT) > 154 N(AGT), which is considered to be a natural variant as reported in References 96,97. Thus, the LBR sequencing analyses revealed no information that could indicate an impaired function of the protein. However, there are a number of entries in GenBank and UniProt databases linked to the human SUN1 protein. The longest protein-coding SUN1 transcript in Ensembl database—SUN1-001 ENST00000405266, which corresponds to an 822-aa protein—was used in silico to design the primers for PCR amplification. The sizes of expected DNA fragments are shown in Figure 7A, and the PCR products

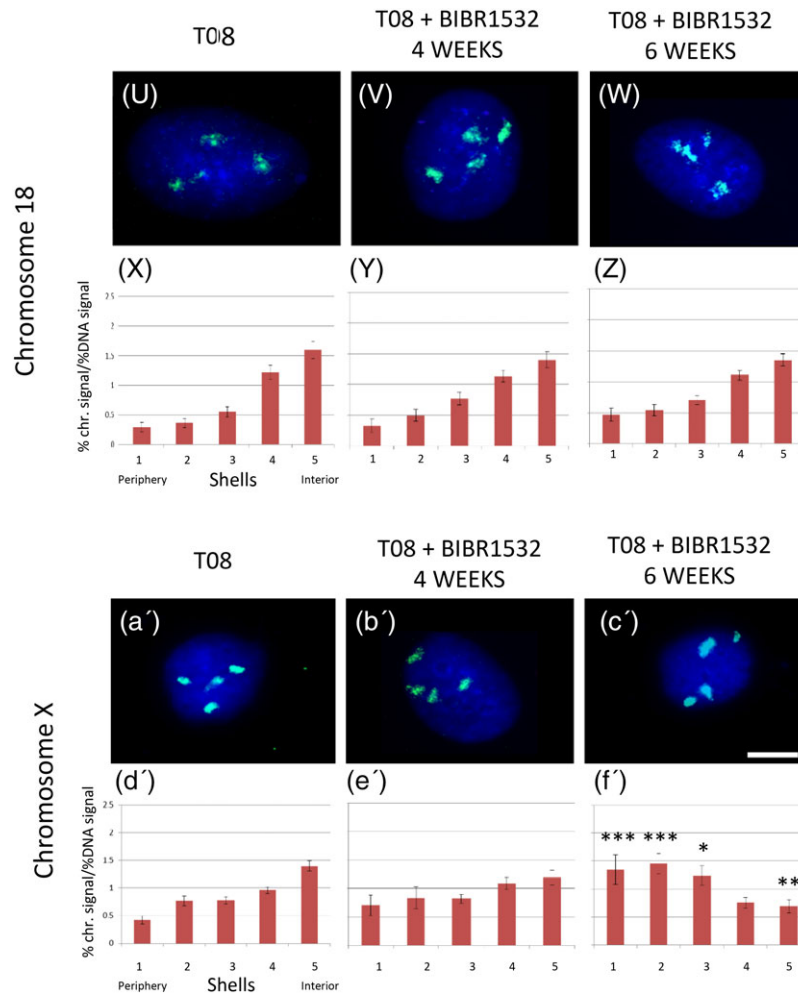


**FIGURE 5** Continued [Color figure can be viewed at [wileyonlinelibrary.com](http://wileyonlinelibrary.com)]

amplified from the cDNA from T08 cells using of the pairs of primers, as well as the full-length ORF are analyzed in Figure 7B. The amplification using the SUN1.f2 and SUN.r2 primers produced an abundant band of the size matching the designed C-terminal half of the SUN1 ORF. The SUN1.f1 and SUN1.r1 primers generated several bands indicating the presence of isoforms that are different at their N-termini. Interestingly, the most abundant band migrated well above the 1500 bp DNA marker, suggesting that the SUN1 protein from T08 cells is encoded by the mRNA which is longer than the longest protein-coding SUN1 transcript in Ensembl database. N-terminal clones were different from the canonical SUN1 sequences. Two clones, containing the longest PCR product (Figure 7B, lane 5), matched SUN1 isoform-9 annotated without experimental confirmation on the UniProt database, and one clone, corresponding to the shorter, less abundant PCR product (Figure 7, lane 5), is a novel SUN1 isoform. We also found the H118 (CAC) > Y118 (TAC) substitution which could be considered as a natural variant.<sup>98</sup> Further analysis of both of these genes by PCR amplification and sequencing revealed that there is no mutation in LBR within exons. Therefore, we have found, in the T08 cells, an isoform of SUN1 that has only ever been suggested to exist in theory (Figure 8). Exons 4 and 5 are both missing which compares to isoform-9. This isoform would correspond to the lower molecular weight PCR fragment in Figure 7 whereas the higher molecular weight fragment matches the isoform-9. We did not attempt to quantify the

expression of different isoform, but a relative abundance of bands in Figure 7B would match the 2:1 ratio of the sequenced clones.

The novel SUN1 isoform would not be recognized by the antibodies employed here and so its presence, rather than typical SUN1, may be responsible for lack of chromosome X at the nuclear periphery and the genomic instability once the atypical HGPS cells had been immortalized with hTERT. Furthermore, full exome sequencing did not reveal any other variations in known integral membrane proteins (data to be deposited in figshare at Brunel University London as an open access data set).

## 4 | DISCUSSION

This study has revealed that by immortalizing normal primary human dermal fibroblasts with hTERT, interphase chromosome positioning is affected in two cell-lines, one from an HGPS primary line and a normal control primary fibroblast line. In young proliferating primary cells, the gene-poor chromosome 18 territories are normally located at the nuclear periphery, with a number of attachments through lamina-associated domains (LADs). However, in cells that are resting in replicative senescence or quiescence chromosome 18 is located in the nuclear interior.<sup>20</sup> In this study, we demonstrate for the first time that chromosome 18 territories are found in the nuclear interior of normal

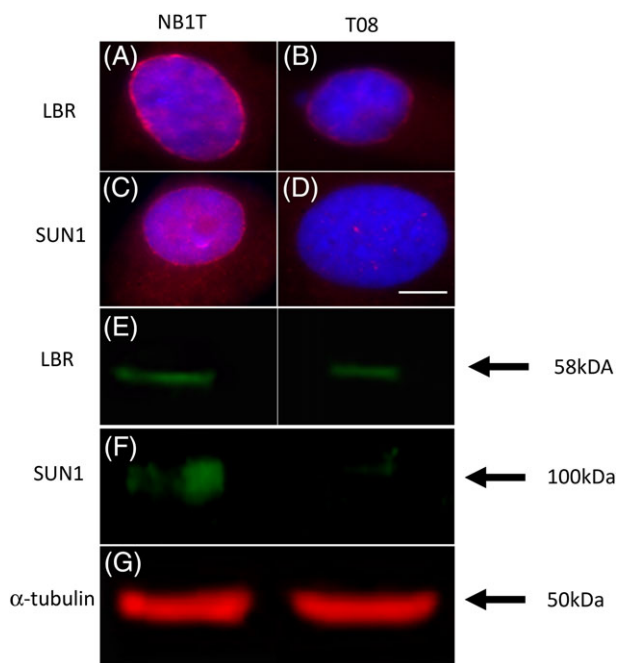


**FIGURE 6** Expression differences of nuclear envelope proteins. Representative images of lamin B receptor (red), SUN1 (red) in NB1T (A, C, respectively) and T08 cells (B, D, respectively). Nuclear DNA is counter-stained with DAPI (blue). Scale bar = 5  $\mu$ m. Samples of NB1T control and atypical HGPS (T08) cell lines in 3X SDS sample buffer were resolved on 10% SDS-PAGE gels, and anti-SUN1 and anti-LBR antibodies were used to identify SUN1 and LBR in western blots. All samples were loaded equally, with  $2 \times 10^5$  cells per lane.  $\alpha$ -tubulin was visualized to normalize the level of proteins [Color figure can be viewed at [wileyonlinelibrary.com](http://wileyonlinelibrary.com)]

proliferating control cells, the only change being that they have been immortalized by hTERT. This interior location is also observed in the two immortalized HGPS cell lines and corresponds to that previously observed nuclear position for chromosome 18 territories in HGPS

cells.<sup>40,66,71</sup> Another novel finding of this study is that chromosome X territories are located in the nuclear interior in the T08 HGPS cell line. This line does not contain the classical G608G lamin A mutation and so does not express progerin, and displays lamin A expression (Supporting Information Figure S6).

We propose these unusual positions of chromosomes 18 and X in the hTERT-immortalized cells must be due to the elongation of the telomere repeats in the cells because, with the erosion of the telomere length by the drug BIBR1532, both of these chromosomes in the NB1Ts and T08s, respectively, are relocated back to the nuclear periphery. The timing of this is coincident with telomeres becoming on average of similar length to the control cells at an early passage number. Thus, a conclusion from this work must be that elongated telomeres found in immortalized and transformed cells leads to whole chromosome repositioning in proliferating cells. As all of the chromosome positioning was performed on proliferating cells, positive for Ki67, no cells that were either senescent or quiescent could have been analyzed. Therefore, the reactivation of telomerase in cancer cells could be responsible for changes of specific chromosome positioning (for overview see 20,21: especially of chromosome 18 and the subsequent consequences of genome reorganization). Consequently, this finding that chromosomes are repositioned in interphase is a concerning finding and has implications both for carcinogenesis and for hTERT-immortalized cells being used for modeling *in vivo* conditions.

Most interestingly, immortalizing the AG08466 cell line to give us the T08 line resulted in tetraploid cells from a near normal karyotype indicative of genomic instability (Supporting Information Table S1). Extra copies of chromosomes have been shown to go to the same nuclear compartments<sup>33,99</sup> and this is what we have observed as well in this study. Thus, the number of individual chromosomes should not change the overall probabilistic chromosome position.

The chromosome repositioning and aneuploidy of chromosome 18 in the T08s does not appear to be due to any issues with lamin B2,

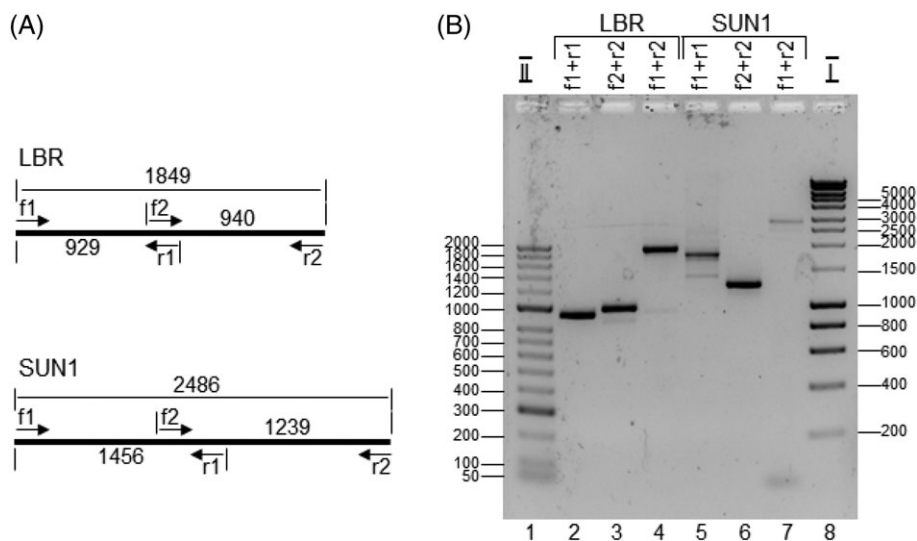


**FIGURE 7** Cloning of the LBR and SUN1 fragments generated from cDNA of HGPS T08 cells for sequencing analysis. Schematics of the *in silico* designed DNA fragments generated using primers designated by the arrows (A). The expected sizes of DNA fragments are shown in numbers of base-pairs. (B) Gel electrophoresis analysis of LBR fragments (lanes 2, 3, 4) and the SUN1 fragments (lanes 5, 6, 7) amplified from cDNA of T08 cells using the pairs of primers indicated above the lanes. Lanes 1 and 8 are the DNA molecular weight markers, BIOLINE Hyperladder II and I, respectively. The sizes of the DNA markers in base-pairs are shown on the left and the right side

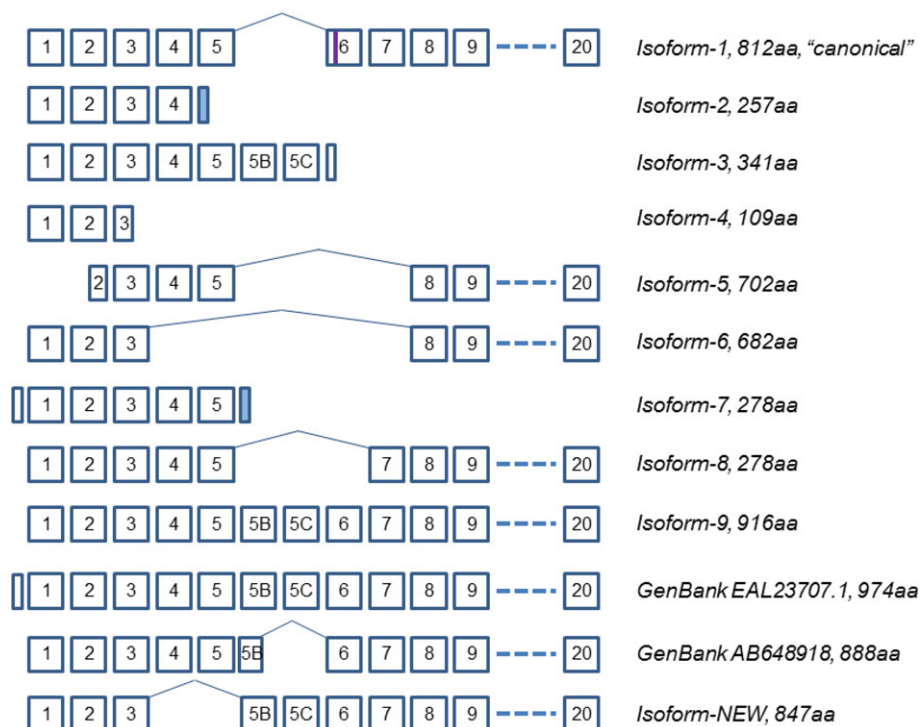


**FIGURE 8** Schematic presentation of the human SUN1 isoforms annotated under O94901 at UniProt database as well as other relevant sequences deposited into GenBank. A novel isoform identified in this work is shown at the bottom of the schematic. The exon numbers are annotated in Ensembl database for SUN1-001 transcript (ENSG00000164828). The exons are shown as boxes with the corresponding number. The exons 10–19 are presented as a dash line as they are identical for all the isoforms containing the C-terminal half. A vertical bar in exon 6 represents the 10-aa peptide missing in the canonical isoform-1 that was identified during phosphoproteomics analysis by<sup>93</sup> [Color figure can be viewed at [wileyonlinelibrary.com](http://wileyonlinelibrary.com)]

which might have led to genomic instability,<sup>100</sup> as lamin B2 is found in good amounts in the nuclear envelope (Supporting Information Figure S5), although we do see a possible mutation in whole exome sequencing. However, LBR levels are affected in T08 cells and could be responsible for problems with chromosome anchorage as LBR is known to bind chromatin.<sup>101</sup> We have also seen chromosome and gene mislocalization in breast cancer cells that are missing LBR<sup>102</sup> and have revealed that LBR has a role to play in development of breast cancer.<sup>103</sup> Indeed, lack of LBR has been linked to chromatin mislocalization before.<sup>104</sup> However, in T08 we have found that there was a lack of SUN1 at the nuclear envelope but after some genomic analyses we have found a SUN1 isoform lacking exons 4 and 5B and none of the isoform 1 normally found. The gene encoding SUN1 protein is located on chromosome 7 (Ensembl database, ENSG00000164828). Exons 1 to 20 are annotated for the longest protein coding SUN1 transcript in Ensembl database—SUN1-001 ENST00000405266, which corresponds to the 822-aa protein—that is 10 aa longer than the canonical SUN1 isoform-1 of 812 aa deposited into UniProt database O94901. The 10-aa peptide TAAHSQSPRL (exon 6) missing in the canonical isoform-1 was experimentally identified during phosphoproteomics analysis via the presence of the phosphoserine in this peptide.<sup>105</sup> There are nine isoforms of SUN1 protein annotated in UniProt database under the entry O94901 that are schematically depicted in Figure 8. The isoforms -2, -3, -4, -5, -6 and -7 were characterized by Ota et al.<sup>97</sup>; the existence of isoforms -2, -7 and 8 was also reported by Gerhard et al.<sup>106</sup>; and isoform-4 was confirmed by Bechtel et al.<sup>107</sup>; the 10-aa phosphopeptide identified by Olsen et al.<sup>105</sup> is a signature of the isoform-9. However, according to UniProt database, no

experimental confirmation available for isoforms -2, -3, -6, -7, -8, -9 is available. In addition, there are two GenBank entries relevant to the SUN1 protein-AB648918.1 (direct submission of [Nishioka, Y. and Hieda, M., 2011, “Novel function of SUN1”, unpublished] is identical to isoform-9 but the exon 5C is absent. EAL23707.1, the longest SUN1 protein coding sequence (974-aa) deposited into GenBank, is the result of so-called conceptual translation, of the chromosome 7 sequence.<sup>108</sup> This sequence is identical to the isoform-9 from Uniprot, but it also contains additional 58-aa at the N-terminus that are present in the isoform-7. The presence of these 58-aa is very unlikely as this could only occur if noncanonical splice sites are used. To analyze the cDNA sequence of SUN1 from T08 cells, we amplified the N-terminal part encompassing exons 1–12 and the C-terminus—exons 11–20; cloned them and sequenced three clones from each set. All the C-terminal sequences were identical to those sequences which were already deposited in GenBank supporting the notion the C-terminal half is not subjected to alternative splicing. Two clones for the N-terminal half aligned perfectly to the isoform-9, including the 10-aa peptide identified by Olsen et al.<sup>105</sup> The isoform-9 is longer compared to the canonical isoform-1 and contains two additional exons which we designated as exons 5B and 5C. Both exons are nicely spaced between exon 5 and exon 6 and are surrounded by nearly perfect splicing signals. Thus, we provide the experimental confirmation for existence of the isoform-9.

It is possible that the lack of canonical SUN1 and presence of a new isoform was responsible for the lack of LBR at the nuclear envelope as it is expressed (Figures 6B and 8). Furthermore, the presence of the novel isoform of SUN1 in combination with

elongated telomeres could be why chromosome X was not anchored at the periphery but can return after telomere erosion. In addition, the combination of elongated telomeres and the presence of the SUN1 isoform 9 has seemed to generate genomic instability in the T08s. This is not the first time that SUN1 has been implicated in genome instability since studies in *Dictyostelium*<sup>109</sup> and mouse<sup>110</sup> have revealed SUN1's role in maintaining genomic health and is known to interact with telomeres<sup>56,111–114</sup> and nuclear envelope flexibility.<sup>115</sup> Obviously, further studies are required to reveal the relationship of telomeres and the SUN1 isoform 9.

How might this relocation of chromosomes be elicited? It is possible that expansion of the telomeres changes their epigenetic fingerprint and so they are no longer able to interact with nuclear lamins in the same way and do not become attached to the nuclear envelope in nuclear reformation after mitosis.<sup>116</sup> It could also be that elongated telomeres may load up more nucleolar proteins at mitosis due to the extended repeats and then end up being taken into the nuclear interior and embedded within nucleoli. Ki67, a nucleolar protein, has been observed in mitotic chromosomes<sup>117,118</sup> associated with telomeres with these genomic regions being then coalesced with the rebuilding nucleoli.<sup>119</sup> This would imply in this situation that all telomeres and chromosomes would be associated with nucleoli and away from the nuclear periphery but DAPI distributions across the five shells are normal and so is unlikely. A further question has to be why do chromosomes behave differently within the T08 cells, such that chromosome 10 does not differ as much as the X chromosomes. We have found dramatic differences in the some heterochromatin marks and proteins (Supporting Information Figure S7). Indeed, HP1 $\alpha$  is missing totally in T08 cells and since it is located on X chromosomes, specifically the Barr body,<sup>120</sup> its lack may well affect chromosomes binding at the nuclear envelope. Indeed, HP1 $\alpha$  binds to LBR, anchoring chromatin at the nuclear periphery, with both proteins compromised in these cells in addition to elongated telomeres there may well be a binding issue. Lamin B is implicated in altering genome organization in progeria cells—indeed gene-rich areas of the genome are more prevalent at nuclear sites lacking B-type lamins.<sup>121</sup> However, in the T08 cells there is not an abnormal amount of B-type lamin (Supporting Information Figure S3).

When the parental cell-line AGO8466 was subjected to exome sequencing and the data analyzed, mutations in two DNA repair enzymes were revealed, *MSH4* and *HELQ* (see Supporting Information Figure S8). These mutations could affect the amount of protein present for these two genes because for *MSH4* there is a predicted loss of the acceptor splice site for exon 10 with the likely effect being the exclusion of exon 10 resulting in a frameshift and an early stop codon. For *HELQ*, there are two possible effects of that mutation—either the continued usage of the donor splice site with a frameshift caused by the deletion of 10 nucleotides or the loss of the donor splice site with a possible intron retention and stop codon after 16 codons (Supporting Information Figure S8). Further investigation into the effect of these mutations is also warranted and such mutations may also be implicated in the genomic instability observed when the cells were immortalized. Furthermore, the cell lines associated with this patient diagnosis may perhaps be described as HGPS-like progeroid disease, although SUN1 interactions with lamin A are involved in progeric laminopathies.<sup>92,93</sup>

BIBR1532 has been used in many studies to cause apoptosis of cancer cells with extended telomeres. However, in our study we used a low dose that did not induce noticeable amounts of cell death, but was able to produce cell cultures that were passaged normally over the 6–8-week period. Instead, we found shorter telomeres and senescent cells, determined using anti-Ki67 as a proliferation marker in the presence of BIBR1532. One interesting exploitation of our findings could be that at a low dose, BIBR1532 could work as a companion drug for chemotherapy working through the telomeres to result in the restoration of a more normal spatial positioning of chromosomes, allowing their spatio-epigenetics responses to be more like nonimmortalized cells.

## ACKNOWLEDGMENTS

The authors would like to thank Dr. Paola Vagnarelli for the use of HP1 $\alpha$  antibodies and her LiCor western blot analysis system, Dr Ines Castro for helping in the western blot analysis, Prof. Nicola Levy for the initial screening of the cell line AGO8466 to check for the G608G mutation in lamin A and Prof Wendy Bickmore for the chromosome positioning erosion analysis software.

## ORCID

Joanna M. Bridger  <https://orcid.org/0000-0003-3999-042X>

## REFERENCES

- Rodier F, Campisi J. Four faces of cellular senescence. *J Cell Biol.* 2011;192(4):547–556.
- Campisi J. Senescent cells, tumor suppression, and organismal aging: good citizens, bad neighbours. *Cell.* 2005;120(4):513–522.
- Blackburn EH. Telomeres and telomerase: their mechanisms of action and the effects of altering their functions. *FEBS Lett.* 2005;579(4):859–862.
- Blackburn EH. Telomere states and cell fates. *Nature.* 2000;408(6808):53–56.
- Campisi J. Aging, cellular senescence, and cancer. *Annu Rev Physiol.* 2013;75:685–705.
- Ramirez RD, Morales CP, Herbert BS, et al. Putative telomere-independent mechanisms of replicative aging reflect inadequate growth conditions. *Genes Dev.* 2001;15(4):398–403.
- Lowe D, Horvath S, Raj K. Epigenetic clock analyses of cellular senescence and ageing. *Oncotarget.* 2016;7(8):8524–8531.
- Wu X, Cao N, Fenech M, Wang X. Role of Sirtuins in maintenance of genomic stability: relevance to cancer and healthy aging. *DNA Cell Biol.* 2016;35:542–575.
- Waaiker ME, Parish WE, Strongitharm BH, et al. The number of p16INK4a positive cells in human skin reflects biological age. *Aging Cell.* 2012;11(4):722–725.
- Kill IR, Faragher RGA, Lawrence K, Shall S. The expression of proliferation-dependent antigens during the lifespan of normal and progeroid human fibroblasts in culture. *J Cell Sci.* 1994;107(Pt 2):571–579.
- Kilian A, Bowtell DD, Abud HE, et al. Isolation of a candidate human telomerase catalytic subunit gene, which reveals complex splicing patterns in different cell types. *Human Mol Genet.* 1997;6(12):2011–2019.
- Weinrich SL, Pruzan R, Ma L, et al. Reconstitution of human telomerase with the template RNA component hTR and the catalytic protein subunit hTRT. *Nat Genet.* 1997;17(4):498–502.
- Feng J, Funk WD, Wang SS, et al. The RNA component of human telomerase. *Science (New York, NY).* 1995;269(5228):1236–1241.

14. Bodnar AG, Ouellette M, Frolkis M, et al. Extension of life-span by introduction of telomerase into normal human cells. *Science*. 1998; 279(5349):349-352.
15. Ouellette MM, McDaniel LD, Wright WE, Shay JW, Schultz RA. The establishment of telomerase-immortalised cell lines representing human chromosome instability syndromes. *Human Mol Genet*. 2009; 9(3):403-411.
16. Aubert G, Lansdorp PM. Telomeres and aging. *Physiol Rev*. 2008; 88(2):557-579.
17. Hastie ND, Dempster M, Dunlop MG, Thompson AM, Green DK, Allshire RC. Telomere reduction in human colorectal carcinoma and with ageing. *Nature*. 1990;346(6287):866-868.
18. Armbruster BN, Etheridge KT, Broccoli D, Counter CM. Putative telomere-recruiting domain in the catalytic subunit of human telomerase. *Mol Cell Biol*. 2003;23(9):3237-3246.
19. Fakhoury J, Marie-Egyptienne DT, Londoño-Vallejo JA, Autexier C. Telomeric function of mammalian telomerases at short telomeres. *J Cell Sci*. 2010;123(Pt 10):1693-1704.
20. Bridger JM, Arican-Gotkas HD, Foster HA, et al. The non-random repositioning of whole chromosomes and individual gene loci in interphase nuclei and its relevance in disease, infection, aging, and cancer. In: Schirmer EC, de las Heras J, eds. *Cancer Biology and the Nuclear Envelope*. Vol 773. New York: Springer; 2014:263-279.
21. Bourne G, Moir C, Bikkul U, et al. Interphase chromosome behavior in normal and diseased cells. In: Yurov Y, Vorsanova S, Iourov I, eds. *Human Interphase Chromosomes*. New York: Springer; 2013:9-33.
22. Fritz AJ, Stojkovic B, Ding H, et al. Wide-scale alterations in interchromosomal organization in breast cancer cells: defining a network of interacting chromosomes. *Hum Mol Genet*. 2014;23(19):5133-5146.
23. Marella NV, Bhattacharya S, Mukherjee L, Xu J, Berezney R. Cell type specific chromosome territory organization in the interphase nucleus of normal and cancer cells. *J Cell Physiol*. 2009;221(1):130-137.
24. Meaburn KJ, Gudla PR, Khan S, Lockett SJ, Misteli T. Disease-specific gene repositioning in breast cancer. *J Cell Biol*. 2009;187(6):801-812.
25. Bell ES, Lammerding J. Causes and consequences of nuclear envelope alterations in tumour progression. *Eur J Cell Biol*. 2016;95(11):449-464.
26. Cremer T, Cremer M. Chromosome territories. *Cold Spring Harbor Perspect Biol*. 2010;2(3):a003889.
27. Cremer T, Cremer C. Chromosome territories, nuclear architecture and gene regulation in mammalian cells. *Nat Rev Genet*. 2009;37(11):3558-3568.
28. Cremer T, Cremer C. Rise, fall and resurrection of chromosome territories: a historical perspective. Part II. Fall and resurrection of chromosome territories during the 1950s to 1980s. Part III. Chromosome territories and the functional nuclear architecture: experiments and models from the 1990s to the present. *Eur J Histochem*. 2006;50(4):223-272.
29. Gilbert N, Gilchrist S, Bickmore WA. Chromatin organization in the mammalian nucleus. *Int Rev Cytol*. 2005;242:283-336.
30. Bridger JM, Bickmore WA. Putting the genome on the map. *Trends Genet*. 1998;14(10):403-409.
31. Bolzer A, Kreth G, Solovei I, et al. Three-dimensional maps of all chromosomes in human male fibroblast nuclei and prometaphase rosettes. *PLoS Biol*. 2005;3(5):826-842.
32. Boyle S, Gilchrist S, Bridger JM, Mahy NL, Ellis JA, Bickmore WA. The spatial organization of human chromosomes within the nuclei of normal and emerin-mutant cells. *Human Mol Genet*. 2001;10(3):211-219.
33. Croft JA, Bridger JM, Boyle S, Perry P, Teague P, Bickmore WA. Differences in the localization and morphology of chromosomes in the human nucleus. *J Cell Biol*. 1999;145(6):1119-1131.
34. Fraser J, Ferrai C, Chiariello AM, et al. Hierarchical folding and reorganization of chromosomes are linked to transcriptional changes in cellular differentiation. *Molecular Systems Biol*. 2015;11(12):852.
35. Nicodemi M, Pombo A. Models of chromosome structure. *Curr Opin Cell Biol*. 2014;28:90-95.
36. Bickmore WA, van Steensel B. Genome architecture: domain organization of interphase chromosomes. *Cell*. 2013;152(6):1270-1284.
37. Guelen L, Pagie L, Brasset E, et al. Domain organization of human chromosomes revealed by mapping of nuclear lamina interactions. *Nature*. 2008;453(7197):948-951.
38. Mehta IS, Amira M, Harvey AJ, Bridger JM. Rapid chromosome territory relocation by nuclear motor activity in response to serum removal in primary human fibroblasts. *Genome Biol*. 2010;11(1):1-23.
39. Mehta IS, Figgitt M, Clements CS, Kill IR, Bridger JM. Alterations to nuclear architecture and genome behavior in senescent cells. *Ann N Y Acad Sci*. 2007;1100:250-263.
40. Meaburn KJ, Cabuy E, Bonne G, et al. Primary laminopathy fibroblasts display altered genome organization and apoptosis. *Aging Cell*. 2007;6:139-153.
41. Bridger J, Boyle S, Kill IR, Bickmore W. Re-modelling of nuclear architecture in quiescent and senescent human fibroblasts. *Curr Biol*. 2000;10(3):149-152.
42. Bridger JM. Chromobility: the rapid movement of chromosomes in interphase nuclei. *Biochem Soc Trans*. 2011;39(6):1747-1751.
43. Czapiewski R, Robson MI, Schirmer EC. Anchoring a leviathan: how the nuclear membrane tethers the genome. *Front Genet*. 2016;7(82):1-13.
44. Dillinger S, Straub T, Németh A. Nucleolus association of chromosomal domains is largely maintained in cellular senescence despite massive nuclear reorganisation. *PLoS One*. 2017;12(6):e0178821.
45. van Koningsbruggen S, Gierlinski M, Schofield P, et al. High-resolution whole-genome sequencing reveals that specific chromatin domains from most human chromosomes associate with nucleoli. *Mol Biol Cell*. 2010;21(21):3735-3748.
46. Sawyer IA, Sturgill D, Sung M, Hager GL, Dundr M. Cajal body function in genome organization and transcriptome diversity. *Bioessays*. 2016;38(12):1197-1208.
47. Dundr M. Nuclear bodies: multifunctional companions of the genome. *Curr Opin Cell Biol*. 2012;24(3):415-422.
48. Wang Q, Sawyer IA, Sung M, et al. Cajal bodies are linked to genome conformation. *Nat Commun*. 2016;7:1-17.
49. Kind J, Van Steensel B. Stochastic genome-nuclear lamina interactions. *Nucleus*. 2014;5(2):124-130.
50. Lund E, Oldenburg AR, Delbarre E, et al. Lamin A/C-promoter interactions specify chromatin state-dependent transcription outcomes. *Genome Res*. 2013;23(10):1580-1589.
51. Luderus ME, van Steensel B, Chong L, Sibon OC, Cremers FF, de Lange T. Structure, subnuclear distribution, and nuclear matrix association of the mammalian telomeric complex. *J Cell Biol*. 1996;135(4):867-881.
52. Raz V, Vermolen BJ, Garini Y, et al. The nuclear lamina promotes telomere aggregation and centromere peripheral localization during senescence of human mesenchymal stem cells. *J Cell Sci*. 2008;121:4018-4028.
53. Schmitt J, Benavente R, Hodzic D, Hoog C, Stewart CL, Alsheimer M. Transmembrane protein Sun2 is involved in tethering mammalian meiotic telomeres to the nuclear envelope. *Proc Natl Acad Sci U S A*. 2007;104(18):7426-7431.
54. Burla R, Carcuro M, Torre ML, et al. The telomeric protein AKTIP interacts with A- and B-type lamins and is involved in regulation of cellular senescence. *Open Biol*. 2016;6(8):1-11.
55. Burla R, Carcuro M, Raffa GD, et al. AKTIP/Ft1, a new Shelterin-interacting factor required for telomere maintenance. *PLoS Genet*. 2015;11(6):1-24.
56. Ding X, Xu R, Yu J, Xu T, Zhuang Y, Han M. SUN1 is required for telomere attachment to nuclear envelope and gametogenesis in mice. *Dev Cell*. 2007;12(6):863-872.
57. Xu R, Alsheimer M. Analysis of meiosis in SUN1 deficient mice reveals a distinct role of SUN2 in mammalian meiotic LINC complex formation and function. *Nucleus*. 2014;10(2):1-9.
58. Godwin LS. The role of lamin A and emerin in mediating Genome organisation [PhD Thesis]. London: Brunel University London; 2010.
59. De Lange T. Human telomeres are attached to the nuclear matrix. *EMBO J*. 1992;11(2):717-724.
60. Dechat T, Gajewski A, Korbei B, et al. LAP2alpha and BAF transiently localize to telomeres and specific regions on chromatin during nuclear assembly. *J Cell Sci*. 2004;117:6117-6128.

61. Gonzalo S, Eissenberg JC. Tying up loose ends: telomeres, genomic instability and lamins. *Curr Opin Genet Dev.* 2016;37:109-118.
62. Gonzalo S, Jaco I, Fraga MF, et al. DNA methyltransferases control telomere length and telomere recombination in mammalian cells. *Nat Cell Biol.* 2006;8(4):416-424.
63. Gonzalo S, Blasco MA. Role of Rb family in the epigenetic definition of chromatin. *Cell Cycle.* 2005;4(6):752-755.
64. Kubben N, Adriaens M, Meuleman W, Voncken JW, van Steensel B, Misteli T. Mapping of Lamin A- and progerin-interacting genome regions. *Chromosoma.* 2012;121:447-464.
65. Zuleger N, Robson MI, Schirmer EC. The nuclear envelope as a chromatin organizer. *Nucleus.* 2011;2(5):339-349.
66. Mehta IS, Eskiw CH, Arican HD, Kill IR, Bridger JM. Farnesyltransferase inhibitor treatment restores chromosome territory positions and active chromosome dynamics in Hutchinson-Gilford progeria syndrome cells. *Genome Biol.* 2011;12(8):1-23.
67. Mewborn SK, Puckelwartz MJ, Abusneineh F, et al. Altered chromosomal positioning, compaction, and gene expression with a lamin A/C gene mutation. *PLoS One.* 2010;5(12):1-13.
68. Shumaker DK, Dechat T, Kohlmaier A, et al. Mutant nuclear lamin A leads to progressive alterations of epigenetic control in premature aging. *Proc Natl Acad Sci U S A.* 2006;103(23):8703-8708.
69. Goldman RD, Shumaker DK, Erdos MR, et al. Accumulation of mutant lamin A causes progressive changes in nuclear architecture in Hutchinson-Gilford progeria syndrome. *Proc Natl Acad Sci U S A.* 2004;101(24):8963-8968.
70. Horvath S, Oshima J, Martin GM, et al. Epigenetic clock for skin and blood cells applied to Hutchinson Gilford Progeria Syndrome and ex vivo studies. *Aging (Albany NY).* 2018;10(7):1758-1775.
71. Bikkul MU, Clements CS, Godwin LS, Goldberg MW, Kill IR, Bridger JM. Farnesyltransferase inhibitor and rapamycin correct aberrant genome organisation and decrease DNA damage respectively, in Hutchinson-Gilford progeria syndrome fibroblasts. *Biogerontology.* 2018;19:579-602. <https://doi.org/10.1007/s10522-018-9758-4>.
72. Wallis CV, Sheerin AN, Green MHL, Jones CJ, Kipling D, Faragher RGA. Fibroblast clones from patients with Hutchinson-Gilford progeria can senesce despite the presence of telomerase. *Exp Gerontol.* 2004;39(4):461-467.
73. Adam-Zahir S, Plowman PN, Bourton EC, Sharif F, Parris CN. Increased gamma-H2AX and Rad51 DNA repair biomarker expression in human cell lines resistant to the chemotherapeutic agents nitrogen mustard and cisplatin. *Chemotherapy.* 2014;60(5-6):310-320.
74. Parsch D, Brassat U, Brummendorf TH, B.T, Fellenberg J. Consequences of telomerase inhibition by BIBR1532 on proliferation and chemosensitivity of chondrosarcoma cell lines. *Cancer Invest.* 2008;26:590-596.
75. Parris CN, Adam Zahir S, Al-Ali H, Bourton EC, Plowman C, Plowman PN. Enhanced  $\gamma$ -H2AX DNA damage foci detection using multimagnification and extended depth of field in imaging flow cytometry. *Cytometry A.* 2015;87:717-723.
76. Foster HA, Estrada-Girona G, Themis M, et al. Relative proximity of chromosome territories influences chromosome exchange partners in radiation-induced chromosome rearrangements in primary human bronchial epithelial cells. *Mutat Res.* 2013;756:66-77.
77. Clements CS, Bikkul U, Ahmed MH, Foster HA, Godwin LS, Bridger JM. Visualizing the spatial relationship of the genome with the nuclear envelope using fluorescence in situ hybridization. In: Shackleton S, Collas P, Schirmer EC, eds. *The Nuclear Envelope: Methods and Protocols.* Vol 1411. New York: Springer; 2016:387-406.
78. Wong HP, Slijepcevic P. Telomere length measurement in mouse chromosomes by a modified Q-FISH method. *Cytogenet Genome Res.* 2004;105(2-4):464-470.
79. McIlrath J, Bouffler SD, Samper E, et al. Telomere length abnormalities in mammalian radiosensitive cells. *Cancer Res.* 2001;61(3):912-915.
80. Ojani M. Relationship between DNA damage response and telomere maintenance [PhD thesis]. London: Brunel University; 2012.
81. Newbold RF. The significance of telomerase activation and cellular immortalization in human cancer. *Mutagenesis.* 2002;17(6):539-550.
82. Meyerson M. Telomerase enzyme activation and human cell immortalization. *Toxicol Lett.* 1998;102:41-45.
83. Counter CM, Meyerson M, Eaton EN, et al. Telomerase activity is restored in human cells by ectopic expression of hTERT (hEST2), the catalytic subunit of telomerase. *Oncogene.* 1998;16(9):1217-1222.
84. Cao K, Blair CD, Faddah DA, et al. Progerin and telomere dysfunction collaborate to trigger cellular senescence in normal human fibroblasts. *J Clin Invest.* 2011;121(7):2833-2844.
85. Bridger JM, Kill IR. Aging of Hutchinson-Gilford progeria syndrome fibroblasts is characterised by hyperproliferation and increased apoptosis. *Exp Gerontol.* 2004;39(5):717-724.
86. Corso C, Parry EM, Faragher RG, Seager A, Green MH, Parry JM. Molecular cytogenetic insights into the ageing syndrome Hutchinson-Gilford Progeria (HGPs). *Cytogenet Genome Res.* 2005;111(1):27-33.
87. Slijepcevic P. Telomere length measurement by Q-FISH. *Methods Cell Sci.* 2011;23(1-3):17-22.
88. Decker ML, Chavez E, Vulto I, Lansdorp P. MTelomere length in Hutchinson-Gilford progeria syndrome. *Mech Ageing Dev.* 2009;130(6):377-383.
89. Barma D, Elayadi A, Falck J, Corey DR. Inhibition of telomerase by BIBR 1532 and related analogues. *Bioorg Med Chem Lett.* 2003;3(7):1333-1336.
90. Haque F, Mazzeo D, Patel JT, et al. Mammalian SUN protein interaction networks at the inner nuclear membrane and their role in laminopathy disease processes. *J Biol Chem.* 2010;285(5):3487-3498.
91. Chi YH, Chen CY, Jeang KT. Reversal of laminopathies: the curious case of SUN1. *Nucleus.* 2012;3(5):418-421.
92. Chen ZJ, Wang WP, Chen YC, et al. Dysregulated interactions between lamin A and SUN1 induce abnormalities in the nuclear envelope and endoplasmic reticulum in progeric laminopathies. *J Cell Sci.* 2014;127(Pt 8):1792-1804.
93. Chen CY, Chi YH, Mutalif RA, et al. Accumulation of the inner nuclear envelope protein Sun1 is pathogenic in progeric and dystrophic laminopathies. *Cell.* 2012;149(3):565-577.
94. McKenna T, Rosengarten Y, Viceconte N, Baek JH, Grochová D, Eriksson M. Embryonic expression of the common progeroid lamin A splice mutation arrests postnatal skin development. *Aging Cell.* 2014;13(2):292-302.
95. Sola Carvajal A, McKenna T, Wallén Arzt E, Eriksson M. Overexpression of Lamin B receptor results in impaired skin differentiation. *PLoS One.* 2015;10(6):e0128917.
96. Schuler E, Lin F, Worman HJ. Characterization of the human gene encoding LBR, an integral protein of the nuclear envelope inner membrane. *J Biol Chem.* 1994;269:11312-11317.
97. Ota T, Suzuki Y, Nishikawa T, et al. Complete sequencing and characterization of 21,243 full-length human cDNAs. *Nat Genet.* 2004;36(1):40-45.
98. Nagase T, Ishikawa K, Nakajima D, et al. Prediction of the coding sequences of unidentified human genes. XI. The complete sequences of 100 new cDNA clones from brain which code for large proteins in vitro. *DNA Res.* 1998;5(5):277-286.
99. Nagele RG, Freeman T, McMorris L, Thomson Z, Kitson-Wind K, Lee H. Chromosomes exhibit preferential positioning in nuclei of quiescent human cells. *J Cell Sci.* 1999;112(Pt 4):525-535.
100. Ranade D, Koul S, Thompson J, Prasad KB, Sengupta K. Chromosomal aneuploidies induced upon Lamin B2 depletion are mislocalized in the interphase nucleus. *Chromosoma.* 2016;126(2):223-244.
101. Ye Q, Worman HJ. Primary structure analysis and lamin B and DNA binding of human LBR, an integral protein of the nuclear envelope inner membrane. *J Biol Chem.* 1994;269(15):11306-11311.
102. Ahmed MH. Discovery and restoration of aberrant nuclear structure and genome behaviour in breast cancer cells', Discovery and restoration of aberrant nuclear structure and genome behaviour in breast cancer cells [PhD thesis]. London: Brunel University; 2013.
103. Wazir U, Ahmed MH, Bridger JM, et al. The clinicopathological significance of lamin A/C, lamin B1 and lamin B receptor mRNA expression in human breast cancer. *Cell Mol Biol Lett.* 2013;18(4):595-611.
104. Solovei I, Wang AS, Thanisch K, et al. LBR and lamin A/C sequentially tether peripheral heterochromatin and inversely regulate differentiation. *Cell.* 2013;512(3):584-598.

105. Olsen JV, Vermeulen M, Santamaria A, et al. Quantitative phosphoproteomics reveals widespread full phosphorylation site occupancy during mitosis. *Sci Signal*. 2010;3:ra3. <https://doi.org/10.1126/scisignal.2000475>.
106. Gerhard DS, Wagner L, Feingold EA, et al. The mammalian gene collection (MGC). *Genome Res*. 2004;4(10B):2121-2127.
107. Bechtel S, Rosenfelder H, Duda A, et al. The full-ORF clone resource of the German cDNA Consortium. *BMC Genomics*. 2007;8:399.
108. Scherer SW, Cheung J, MacDonald JR, et al. Human chromosome 7: DNA sequence and biology. *Science*. 2003;300:767-772.
109. Schulz I, Baumann O, Samereier M, Zoglmeier C, Gräf R. Dictyostelium Sun1 is a dynamic membrane protein of both nuclear membranes and required for centrosomal association with clustered centromeres. *Eur J Cell Biol*. 2009;88(11):621-638.
110. Lei K, Zhu X, Xu R, et al. Inner nuclear envelope proteins SUN1 and SUN2 play a prominent role in the DNA damage response. *Curr Biol*. 2012;22(7):1609-1615.
111. Varas J, Graumann K, Osman K, et al. Absence of SUN1 and SUN2 proteins in *Arabidopsis thaliana* leads to a delay in meiotic progression and defects in synapsis and recombination. *Plant J*. 2015;81(2):329-346.
112. Burke B, Stewart CL. Functional architecture of the cell's nucleus in development, aging, and disease. *Curr Top Develop Biol*. 2014;109:1-52.
113. Crabbe L, Cesare AJ, Kasuboski JM, Fitzpatrick JA, Karlseder J. Human telomeres are tethered to the nuclear envelope during post-mitotic nuclear assembly. *Cell Rep*. 2012;2(6):1521-1529.
114. Gonzalo-Suaraz I, Redwood AB, Gonzalo S. Loss of A-type lamins and genomic instability. *Cell Cycle*. 2009;8:3860-3865.
115. Lu X, Djabali K. Autophagic removal of farnesylated carboxy-terminal lamin peptides. *Cells*. 2018;7(4):E33.
116. Booth DG, Beckett AJ, Molina O, et al. 3D-CLEM reveals that a major portion of mitotic chromosomes is not chromatin. *Mol Cell*. 2016;64:790-802.
117. Booth DG, Takagi M, Sanchez-Pulido L, et al. Ki-67 is a PP1-interacting protein that organises the mitotic chromosome periphery. *Elife*. 2014;3:1-22.
118. Endl E, Gerdes J. Posttranslational modifications of the Ki-67 protein coincide with two major checkpoints during mitosis. *J Cell Physiol*. 2000;182(3):371-380.
119. Bridger JM, Kill IR, Lichter P. Association of pKi-67 with satellite DNA of the human genome in early G1 cells. *Chromosome Res*. 1998;6:13-24.
120. Chadwick BP, Willard HF. Chromatin of the Barr body: histone and non-histone proteins associated with or excluded from the inactive X chromosome. *Hum Mol Genet*. 2003;12(17):2167-2178.
121. Bercht Pflighaar K, Taimen P, Butin-Israeli V, et al. Gene-rich chromosomal regions are preferentially localized in the lamin B deficient nuclear blebs of atypical progeria cells. *Nucleus*. 2015;6(1):66-76.

## SUPPORTING INFORMATION

Additional supporting information may be found online in the Supporting Information section at the end of the article.

**How to cite this article:** Bikkul MU, Faragher RGA, Worthington G, et al. Telomere elongation through hTERT immortalization leads to chromosome repositioning in control cells and genomic instability in Hutchinson-Gilford progeria syndrome fibroblasts, expressing a novel SUN1 isoform. *Genes Chromosomes Cancer*. 2019;58:341-356. <https://doi.org/10.1002/gcc.22711>